(12) LEVEL II

DNA 5304D

AD A089715

RADIO WAVE PROPAGATION IN STRUCTURED IONIZATION FOR SATELLITE APPLICATIONS

Captain Leon A. Wittwer
Radiation and Atmospheric Effects Division
Defense Nuclear Agency
Washington, D.C. 20305

31 December 1979

In-House Report for Period 1 August 1978—1 December 1979

Prepared for
Director
DEFENSE NUCLEAR AGENCY
Washington, D. C. 20305

Destroy this report when it is no longer needed. Do not return to sender.

PLEASE NOTIFY THE DEFENSE NUCLEAR AGENCY, ATTN: STTI, WASHINGTON, D.C. 20305, IF YOUR ADDRESS IS INCORRECT, IF YOU WISH TO BE DELETED FROM THE DISTRIBUTION LIST, OR IF THE ADDRESSEE IS NO LONGER EMPLOYED BY YOUR ORGANIZATION.

UNCLASSIFIED

SECURITY CLASSIFICATION OF THIS PAGE (When Data Entered)

(1) Rept. for 1 Aug 78 - 1 Dec 79

REPORT DOCUMENTATION PAGE

READ INSTRUCTIONS BEFORE COMPLETING FORM

(14) 1. REPORT NUMBER: DNA-5304D

2. GOVT ACCESSION NO.: AD-089715

3. RECIPIENT'S CATALOG NUMBER:

(6) 4. TITLE (and Subtitle): RADIO WAVE PROPAGATION IN STRUCTURED IONIZATION FOR SATELLITE APPLICATIONS

5. TYPE OF REPORT & PERIOD COVERED: In-House Report for Period 1 Aug 78—1 Dec 79

6. PERFORMING ORG. REPORT NUMBER:

7. AUTHOR(s): (10) Captain Leon A. Wittwer

8. CONTRACT OR GRANT NUMBER(s): (12) 74

9. PERFORMING ORGANIZATION NAME AND ADDRESS: Radiation and Atmospheric Effects Division, Defense Nuclear Agency, Washington, D.C. 20305

10. PROGRAM ELEMENT, PROJECT, TASK AREA & WORK UNIT NUMBERS:

11. CONTROLLING OFFICE NAME AND ADDRESS: Director, Defense Nuclear Agency, Washington, D.C. 20305

(11) 12. REPORT DATE: 31 December 1979

13. NUMBER OF PAGES:

14. MONITORING AGENCY NAME & ADDRESS (if different from Controlling Office):

15. SECURITY CLASS (of this report): UNCLASSIFIED

15a. DECLASSIFICATION DOWNGRADING SCHEDULE:

16. DISTRIBUTION STATEMENT (of this Report)

Approved for public release; distribution unlimited.

17. DISTRIBUTION STATEMENT (of the abstract entered in Block 20, if different from Report)

18. SUPPLEMENTARY NOTES

19. KEY WORDS (Continue on reverse side if necessary and identify by block number)

Scintillations	Satellite C^3
Propagation	Radar Propagation
Striations	Fading

20. ABSTRACT (Continue on reverse side if necessary and identify by block number)

Methods are presented which permit the calculation of signal structure properties of satellite signals as they propagate through structured ionization. The primary parameters are the signal decorrelation time, the frequency selective bandwidth, the mean square log amplitude fluctuation, and the mean square arrival angle of the signal. The form of the generalized power spectrum, which characterizes the arriving signal as a function of frequency and delay, is specified in terms of the calculated signal structure

DD FORM 1 JAN 73 1473 EDITION OF 1 NOV 65 IS OBSOLETE

UNCLASSIFIED

SECURITY CLASSIFICATION OF THIS PAGE (When Data Entered)

406762

JOB

20. ABSTRACT (Continued)

parameters. Finally, methods are discussed to generate using Monte Carlo techniques signal structures from the generalized power spectrum, ~~using the generalized power spectrum.~~

PREFACE

The models and algorithms in this paper represent a synthesis of results from different works by several different individuals over the past few years. In particular, I would like to acknowledge the contributions of the following people: Dr. Walter Chesnut and Dr. Charles Rino of SRI International, Dr. K. C. Yeh and his colleagues at the University of Illinois at Urbana, Dr. David Sachs of Science Applications Incorporated, Dr. Roy Hendrick, Mr. Robert Bogusch, Dr. Dennis Knepp of Mission Research Corporation, Dr. Clifford Prettie of Berkeley Research Associates, and Dr. E. J. Fremouw of Physical Dynamics Incorporated.

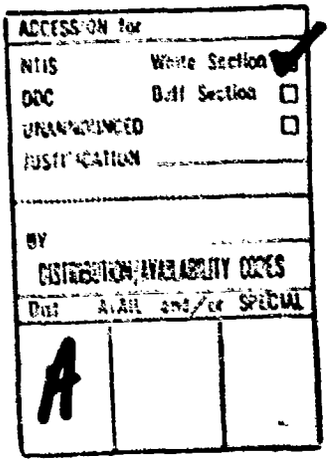

TABLE OF CONTENTS

LIST OF ILLUSTRATIONS

RADIO WAVE PROPAGATION IN STRUCTURED IONIZATION FOR SATELLITE APPLICATIONS

1. INTRODUCTION

The fundamental objectives of the DNA radio wave propagation community have been to determine a necessary and sufficient representation of structured ionization for propagation calculations, to characterize the resulting scintillated signal structures, and to develop methods to make available scintillated signals for systems analysis and test purposes. These objectives have been met for most practical applications.

It was shown in References 1 and 2, that given a sufficiently thick scattering layer, the ionization fluctuation power spectral density was adequate for most propagation purposes. This result was very significant because power spectral densities can be developed from first principles or from measurements. If a more complex representation had been required, then it would have been doubtful that the environment problem could have been adequately solved particularly for these cases where empirical characterization from measurements is not possible.

The characterization of typical scintillated signal structures from the point of view of system performance evaluation has proven particularly simple and useful. The dominant threat to systems both in time and space is from Rayleigh scintillated signals characterized by a generalized power spectrum which is, in turn, parameterized by a small number of variables. This simple characterization permits a separation between detailed environment considerations and system performance evaluations. Put another way,

the "environment" as seen by a system has been reduced to a small number of variables where all the geometric and other complexities of environments have been accounted for. Systems evaluations parameterized by the reasonable ranges of these signal structure parameters thus encompass all reasonably possible environments without calculating explicitly all possible scenarios. The appropriate parameters also constitute "environmental" criteria without the necessity of dealing with specific situations.

The generalized power spectrum, because of its properties, permits easy reconstruction of explicit signals. These signals, in the form of computer data, may be used to exercise software models of satellite systems. The same data can also be used to drive test hardware for testing of satellite hardware against scintillated signals. The remainder of this paper will develop the basic models and algorithms used to implement the concepts just discussed.

2. ENVIRONMENT CHARACTERIZATION

The first step in any propagation study is to characterize the ionization or equivalently the index of refraction fluctuations of the ionospheric propagation environment. Figure 1 illustrates the geometry of a typical satellite link. The index of refraction fluctuations, represented schematically by the curved lines are typically elongated along the magnetic field. $\hat{t}$ is a unit vector along the magnetic field and is a slowly varying function of space since the field lines are curved. The z axis and the $\hat{z}$ unit vector represent the propagation line of sight. The transmitter by definition, is at $z = 0$ and the receiver is at $z = z_t$. The $\hat{r}$ and $\hat{s}$ unit vectors complete with $\hat{t}$ an orthogonal coordinate system that is used to define the structure. The orientation of $\hat{r}$ and $\hat{s}$ is chosen to best represent any anisotropy of the index of refraction structure about the field line. As with $\hat{t}$, $\hat{r}$ and $\hat{s}$ may be slow functions of

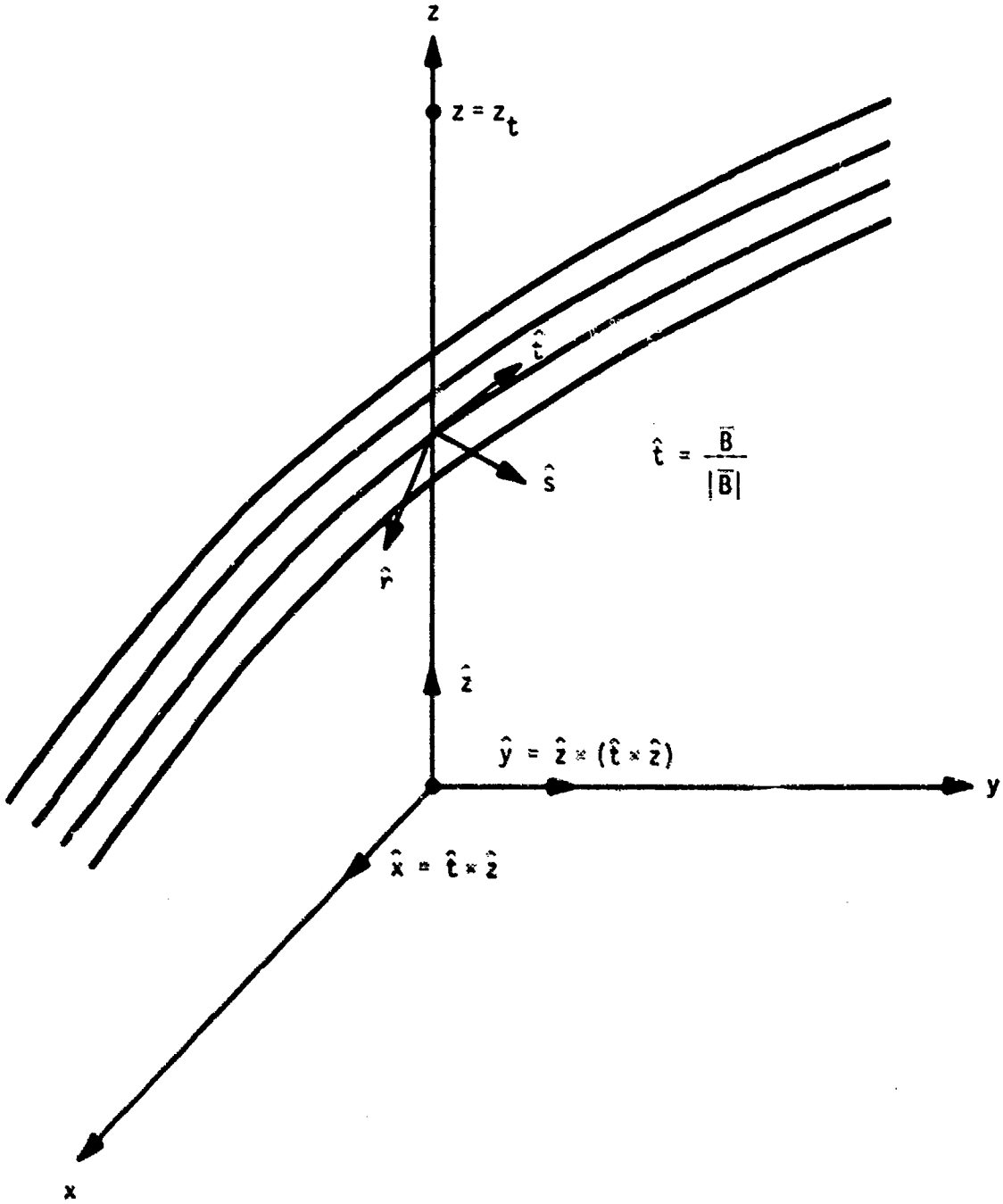

Figure 1. Propagation geometry.

position. In the $\hat{r}$, $\hat{s}$, and $\hat{t}$ system the index of refraction fluctuations are often represented by a power law power spectral density.

$$PSD(K_r,K_s,K_t) = \frac{8\pi^{3/2}\overline{\Delta n_i^2}L_rL_sL_t\Gamma(n)/\Gamma(n-3/2)}{(1+L_r^2K_r^2+L_s^2K_s^2+L_t^2K_t^2)^n} \qquad (1)$$

where

K_r,K_s,K_t = spatial wave numbers

L_r,L_s,L_t = structure outer scales

$\overline{\Delta n_i^2}$ = index of refraction variance

$\Gamma(n)$ = gamma function of argument n

$2n - 2$ = fluctuation spectral index

Both in situ measurements[3-8] and theoretical considerations[9] imply that $n \approx 2$ for ionospheric structured environments. This spectral slope is believed to be caused by the existence of very sharp edged structures. The fluctuation power spectrum is considered a locally homogeneous quantity as discussed by Tatarski[10]. This means that the parameters can be slowly varying functions in any space direction with respect to the spatial scale in that direction.

The structure variation of the index of refraction perpendicular to the $\hat{z}$ axis dominates the propagation effects while the variation parallel to the $\hat{z}$ axis enters only through the strength of the integrated phase variance. Thus Equation 1 must be transformed to a frame with one axis being the $\hat{z}$ axis. These new axes are defined by

$$\hat{x} = \hat{t} \times \hat{z}/|\hat{t} \times \hat{z}| \qquad (2a)$$

$$\hat{y} = \hat{z} \times (\hat{t} \times \hat{z})/|\hat{z} \times (\hat{t} \times \hat{z})| \qquad (2b)$$

Two rotations suffice to accomplish the transformation. First, the $\hat{r}$ axis is rotated about the $\hat{t}$ axis by angle ϕ to become parallel to the $\hat{x}$ axis. ϕ is defined by

$$\hat{t}\sin\phi = \hat{r} \times (\hat{t} \times \hat{z}) \tag{3a}$$

$$\cos\phi = \hat{r} \cdot (\hat{t} \times \hat{z}) \tag{3b}$$

Next, the $\hat{t}$ axis is rotated about the $\hat{x}$ axis by angle Φ into the $\hat{z}$ axis. Φ is defined by

$$\hat{x}\sin\Phi = \hat{t} \times \hat{z} \tag{4a}$$

$$\cos\Phi = \hat{t} \cdot \hat{z} \tag{4b}$$

These transformations can be simplified by defining new effective scale sizes

$$L_x^2 = L_r^2\cos^2\phi + L_s^2\sin^2\phi \tag{5a}$$

$$L_y^2 = (L_r^2\sin^2\phi + L_s^2\cos^2\phi)\cos^2\Phi + L_t^2\sin^2\Phi \tag{5b}$$

$$L_z^2 = (L_r^2\sin^2\phi + L_s^2\cos^2\phi)\sin^2\Phi + L_t^2\cos^2\Phi \tag{5c}$$

$$L_{xy} = (L_s^2 - L_r^2)\cos\Phi\cos\phi\sin\phi \tag{5d}$$

$$L_{xz} = (L_r^2 - L_s^2)\sin\Phi\cos\phi\sin\phi \tag{5e}$$

$$L_{yz} = (L_t^2 - L_r^2\sin^2\phi - L_s^2\cos^2\phi)\cos\Phi\sin\Phi \tag{5f}$$

The final result for the locally homogeneous index of refraction power spectral density is

$$P(K_x,K_y,K_z) = \frac{8\pi^{3/2}\overline{\Delta n_i^2}L_rL_sL_t\Gamma(n)/\Gamma(n-3/2)}{(1 + L_x^2K_x^2 + L_y^2K_y^2 + L_z^2K_z^2 + 2L_{xy}K_xK_y + 2L_{xz}K_xK_z + 2L_{yz}K_yK_z)^n} \tag{6}$$

3. DERIVATION OF SIGNAL STRUCTURE PARAMETERS

The desired signal structure parameters are derivable from the differential phase spectrum. As shown in Appendix A, this spectrum can be attained by multiplying Equation 6 by K^2, where K is the radio signal wave number, and by setting K_z equal to zero. The differential phase spectrum is

$$\frac{dP_\phi(K_x,K_y)}{dz} = \frac{8\pi^{3/2}K^2\overline{\Delta n_i^2}L_rL_sL_t\Gamma(n)/\Gamma(n-3/2)}{(1+L_x^2K_x^2+L_y^2K_y^2+2L_{xy}K_xK_y)^n} \tag{7}$$

The total mean square integrated phase fluctuation is

$$\sigma_\phi^2 = \int_0^{z_t} dz \int_{-\infty}^{\infty} \frac{dK_x}{2\pi} \int_{-\infty}^{\infty} \frac{dK_y}{2\pi} \frac{dP_\phi(K_x,K_y)}{dz} \tag{8a}$$

$$= \int_0^{z_t} dz \frac{d\sigma_\phi^2}{dz} \tag{8b}$$

where $d\sigma_\phi^2/dz$ is

$$\frac{d\sigma_\phi^2}{dz} = \frac{2\pi^{1/2}\Gamma(n-1)}{\Gamma(n-3/2)} K^2\overline{\Delta n_i^2}L_z \tag{9}$$

$$L_z \equiv L_rL_sL_t/(L_x^2L_y^2-L_{xy}^2)^{1/2} \tag{10}$$

L_z is the effective structure scale along the $\hat{z}$ axis. The spectrum in Equation 7 can be rewritten as

$$\frac{dP_\phi(K_x,K_y)}{dz} = \frac{d\sigma_\phi^2}{dz} \frac{4\pi(L_x^2L_y^2-L_{xy}^2)^{1/2}(n-1)}{(1+L_x^2K_x^2+L_y^2K_y^2+2L_{xy}K_xK_y)^n} \tag{11}$$

Equation 11 can be Fourier transformed to

$$\frac{dR_\phi(x,y)}{dz} = \frac{d\sigma_\phi^2}{dz} \frac{\rho^{n-1} K_{n-1}(\rho)}{2^{n-2}\Gamma(n-1)} \tag{12}$$

where

$$\rho^2 = \frac{L_y^2 x^2 - 2L_{xy} xy + L_x^2 y^2}{L_x^2 L_y^2 - L_{xy}^2}$$

Equations 9, 11, and 12 are the fundamental equations from which all of the required propagation quantities can be derived.

The first propagation quantity is the mean square log amplitude fluctuation.[6] This quantity is used as a switch to determine the onset of Rayleigh scintillated signals.

$$\overline{\chi^2} = \int_0^{z_t} dz \int_{-\infty}^{\infty} \frac{dK_x}{2\pi} \int_{-\infty}^{\infty} \frac{dK_y}{2\pi} \sin^2\left[\frac{(K_x^2+K_y^2)(z_t-z)z}{2Kz_t}\right] \frac{dP_\phi(K_x,K_y)}{dz} \tag{13}$$

Let

$$M(z) \equiv \frac{(L_x^2+L_y^2)(z_t-z)z}{Kz_t(L_x^2L_y^2-L_{xy}^2)}$$

The mean square log amplitude fluctuation can be approximately expressed by (see Appendix B)

$$\overline{\chi^2} \equiv \frac{1}{2} \int_0^{z_t} \frac{d\sigma_\phi^2}{dz} \left[\frac{M(z)}{1+M(z)}\right]^{n-1} dz \tag{14}$$

Equation 14 is accurate to about twenty five percent everywhere and usually to within ten percent when $M(z)$ is always small. The applicable range of n is $1.7 \leq n \leq 2.75$.

The remaining signal structure parameters are derivable from the mutual coherence function of $U(z,\bar{r},K)$ where the propagating carrier signal is expressed as

$$E(z,\bar{r},K) = \frac{U(z,\bar{r},K)e^{iK(|\bar{r}|^2 + z^2)^{1/2}}}{z} \tag{15}$$

The mutual coherence function for U is

$$G(z,x,y,\eta) = \overline{U^*(z,\bar{r}_1,K_1)U(z,\bar{r}_2,K_2)} \tag{16}$$

where

$$\eta = (K_2-K_1)/K_2$$

$$x\hat{x} + y\hat{y} = \bar{r}_2 - \bar{r}_1$$

The equation for G is

$$\frac{dG}{dz} = \frac{-i}{2K_2}\left(\frac{\eta}{1-\eta}\right)\left(\frac{d^2G}{dx^2} + \frac{d^2G}{dy^2}\right) - \frac{x}{z}\frac{dG}{dx} - \frac{y}{z}\frac{dG}{dy}$$

$$- \left\{\frac{1}{2}\left[1 + \frac{1}{(1-\eta)^2}\right] - \frac{A_n(x,y)}{1-\eta}\right\}\frac{d\sigma_\phi^2}{dz}\,G \tag{17}$$

where

$$A_n(x,y) = \frac{dR_\phi(x,y)}{dz}\Bigg/\frac{d\sigma_\phi^2}{dz}$$

The differential total integrated phase variance, $d\sigma_\phi^2/dz$ is evaluated at $K = K_2$. Equation 17 includes the effects of spherical waves which permits the transmitter and the receiver to be located arbitrarily with respect to the scattering medium.

Let η equal zero. Then Equation 17 can be written

$$\frac{dG}{dz} = -G\frac{d\sigma_\phi^2}{dz}\left[1 - A_n\left(\frac{zx}{z_t}, \frac{zy}{z_t}\right)\right] \tag{18}$$

with the formal solution

$$G(z,x,y) = e^{-\int_0^z \frac{d\sigma_\phi^2}{dz}\left[1 - A_n\left(\frac{zx}{z_t}, \frac{zy}{z_t}\right)\right] dz} \tag{19}$$

where

$$G(0,x,y) = 1 \quad .$$

The bracket in Equation 19 can be approximated for $\sigma_\phi^2 >> 1$ by

$$1 - A_n\left(\frac{zx}{z_t}, \frac{zy}{z_t}\right) \approx B_n \left(\frac{z\rho}{z_t}\right)^m \tag{20}$$

where

$$m = 2, \quad n \geq 2$$

$$m = 2n - 2, \quad n < 2$$

B_n = constant of order unity

The signal decorrelation distance is defined as the e^{-1} point of G. Thus, for $\sigma_\phi^2 >> 1$,

$$\int_0^{z_t} \frac{d\sigma_\phi^2}{dz} B_n \left(\frac{z\rho_o}{z_t}\right)^m dz \approx 1 \tag{21}$$

defines ρ_o, the decorrelation distance. The decorrelation distance is a function of direction in the x-y plane. The signal decorrelation time is defined as the decorrelation distance in some direction divided by the effective velocity in that same direction. The effective velocity is

$$\bar{V} = \left(\frac{z-z_t}{z}\right) \bar{V}_{tr} + \frac{z_t}{z} \bar{V}_{st} - \bar{V}_{re} \tag{22}$$

where

$\overline{V}_{tr}$ = transmitter velocity

$\overline{V}_{st}$ = index of refraction structure velocity

$\overline{V}_{re}$ = receiver velocity

Let

$$V_x = \overline{V} \cdot \hat{x}$$

$$V_y = \overline{V} \cdot \hat{y}$$

From Equations 20 and 21, the perpendicular decorrelation time, $\tau_\perp$, is

$$\tau_\perp = B(n,\sigma_\phi^2)\left[\int_0^{z_t} \frac{d\sigma_\phi^2}{dz} B_n \left(\frac{z\rho_v}{z_t}\right)^m dz\right]^{-1/m} \qquad (23)$$

where

$$\rho_v^2 = \frac{L_y^2 V_x^2 - 2L_{xy} V_x V_y + L_x^2 V_y^2}{L_x^2 L_y^2 - L_{xy}^2}$$

$$B(n,\sigma_\phi^2) = \text{minimum}\left[1, (-0.34n^2 + 2.51n - 2.00)(\sigma_\phi^2 B_n)^{1/m}\right]$$

The $B(n,\sigma_\phi^2)$ function is used to insure the proper limit on $\tau_\perp$ for small σ_ϕ^2. The decorrelation time, $\tau_\perp$, is with respect to the x-y plane. The signal also decorrelates with time for motion along the $\hat{z}$ axis as a result of the angular scatter of the energy. We will assume for the remainder of this paper that $n \geq 2$ and $\sigma_\phi^2 >> 1$ to continue the development. Restricting n limits the classes of environments but allows a more general geometry.

Let us define a set of fixed axes, $\hat{u}$ and $\hat{v}$, perpendicular to the $\hat{z}$ axis such that $\hat{u} \times \hat{v} = \hat{z}$. At each point on the $\hat{z}$ axis, the rotation angle between the $\hat{x}$ and the $\hat{u}$ axis is defined by

$$\hat{z}\sin\theta = \hat{x} \times \hat{u}$$

$$\cos\theta = \hat{x} \cdot \hat{u}$$

Let

$$L_u^2 = L_y^2\cos^2\theta + L_x^2\sin^2\theta - 2L_{xy}\sin\theta\cos\theta$$

$$L_v^2 = L_x^2\cos^2\theta + L_y^2\sin^2\theta + 2L_{xy}\sin\theta\cos\theta$$

$$L_{uv} = (L_y^2-L_x^2)\sin\theta\cos\theta - L_{xy}(\sin^2\theta-\cos^2\theta)$$

Then

$$\rho^2 = \frac{L_u^2u^2 - 2L_{uv}uv + L_v^2v^2}{L_x^2L_y^2 - L_{xy}^2} \tag{24}$$

The mutual coherence function can be written as

$$G(z_t,u,v) \approx e^{-(C_uu^2+C_vv^2-2C_{uv}uv)} \tag{25}$$

where

$$C_u = \int_0^{z_t} \frac{d\sigma_\phi^2}{dz} B_n\left[\left(\frac{z}{z_t}\right)^2 \frac{L_u^2}{L_x^2L_y^2-L_{xy}^2}\right]dz \tag{26a}$$

$$C_v = \int_0^{z_t} \frac{d\sigma_\phi^2}{dz} B_n\left[\left(\frac{z}{z_t}\right)^2 \frac{L_v^2}{L_x^2L_y^2-L_{xy}^2}\right]dz \tag{26b}$$

$$C_{uv} = \int_0^{z_t} \frac{d\sigma_\phi^2}{dz} B_n\left[\left(\frac{z}{z_t}\right)^2 \frac{L_{uv}}{L_x^2L_y^2-L_{xy}^2}\right]dz \tag{26c}$$

Now, finally, we rotate the u-v coordinates to remove the cross term in G. Let

$$\tan(2\varepsilon) = \frac{2C_{uv}}{C_u - C_v} \tag{27}$$

$$p = u\cos\varepsilon - v\sin\varepsilon \tag{28a}$$

$$q = u\sin\varepsilon + v\cos\varepsilon \tag{28b}$$

$$C_p = \frac{1}{2}\left[C_u+C_v+((C_u-C_v)^2+4C_{uv}^2)^{1/2}\right] \tag{29a}$$

$$C_q = \frac{1}{2}\left[C_u+C_v-((C_u-C_v)^2+4C_{uv}^2)^{1/2}\right] \tag{29b}$$

Then

$$G(z_t,p,q) = e^{-(C_p p^2+C_q q^2)} \tag{30}$$

The parallel signal decorrelation time is defined as

$$\tau_{\parallel} = \frac{3.7K}{(C_p^{2/3}+C_q^{2/3})^{3/2}\left|(\bar{V}_{re}-\bar{V}_{st})\cdot\hat{z}\right|} \tag{31}$$

The final decorrelation time is

$$\tau_o = \text{minimum}(\tau_{\perp},\tau_{\parallel}) \tag{32}$$

The signal power spectrum that is most consistent with the proceeding development is

$$P_s(f) = \sqrt{\pi}\,\tau_o e^{-(\pi f\tau_o)^2} \tag{33}$$

Occasionally, the following form is used to be conservative when $n = 2$.

$$P_s(f) = \frac{\pi\tau_o/1.66}{\left(1+\left(\frac{2\pi\tau_o f}{1.66}\right)^2\right)^{3/2}} \tag{34}$$

Equation 25 can be Fourier transformed resulting in the energy angle of arrival spectrum.

$$P_\theta(\theta_v,\theta_u) = \frac{K^2 e^{-\frac{K^2}{4}\left[\frac{C_u\theta_v^2+2C_{uv}\theta_u\theta_v+C_v\theta_u^2}{C_uC_v-C_{uv}^2}\right]}}{4\pi(C_uC_v-C_{uv}^2)^{1/2}} \tag{35}$$

or in the $\hat{p}$-$\hat{q}$ frame

$$P_\theta(\theta_p,\theta_q) = \frac{K^2}{4\pi(C_pC_q)^{1/2}} e^{-\frac{K^2}{4}\left(\frac{\theta_p^2}{C_p}+\frac{\theta_q^2}{C_q}\right)} \tag{36}$$

where both angular distributions are normalized such that

$$\int_{-\infty}^{\infty} d\theta_v \int_{\infty}^{\infty} d\theta_u \; P_\theta(\theta_v,\theta_u) = 1 \tag{37a}$$

$$\int_{-\infty}^{\infty} d\theta_p \int_{\infty}^{\infty} d\theta_q \; P_\theta(\theta_p,\theta_q) = 1 \tag{37b}$$

The final parameter to be calculated is the variance of the signal energy arrival time. Using a formalism originally developed by Yeh and Liu[11] the effective energy arrival time variance is defined as

$$\sigma_t^2 = \frac{\sigma_{\phi R}^2}{K^2c^2} + \frac{1}{K^4c^2}\int_0^{z_t}\frac{dz'}{z'^2}\int_0^{z'}\frac{dz}{z^2}\left[I_u^2(z)+I_v^2(z)+2I_{uv}^2(z)\right] \tag{38}$$

where

$$I_u(z') = \int_0^{z'} \frac{d\sigma_\phi^2}{dz}\frac{2B_n z^2 L_u^2}{L_x^2L_y^2 - L_{xy}^2}\,dz$$

$$I_v(z') = \int_0^{z'} \frac{d\sigma_\phi^2}{dz}\frac{2B_n z^2 L_v^2}{L_x^2L_y^2 - L_{xy}^2}\,dz$$

$$I_{uv}(z') = \int_0^{z'} \frac{d\sigma_\phi^2}{dz}\frac{2B_n z^2 L_{uv}}{L_x^2L_y^2 - L_{xy}^2}\,dz$$

$\sigma^2_{\phi R}$ is the Rayleigh phase variance derived in Appendix B. It is used to insure that σ^2_t includes only the time delay effects associated with the Rayleigh portion of the signal. The frequency selective bandwidth is defined

$$f_o = 1/2\pi\sigma_t \tag{39}$$

This completes the development of the basic signal structure parameters. In the following, these parameters will be used to define the generalized signal power spectrum.

4. THE GENERALIZED POWER SPECTRUM

Let us assume that the thickness of the scattering layer, z_s, is small compared to the distance from the layer to the receiver and to the transmitter. This is modeled mathematically by letting

$$\frac{d\sigma^2_\phi}{dz} = \sigma^2_\phi \delta(z-z_1) \tag{40}$$

where $\delta(z)$ is the Dirac delta function and z_1 marks the center of the scattering layer. Then

$$G(z_t,p,q,\Delta f) = \frac{1}{(1-i\Delta f/f'_p)^{1/2}(1-i\Delta f/f'_q)^{1/2}}$$

$$\exp\left[-\frac{\sigma^2_\phi}{2}\left(\frac{\Delta f}{f_2}\right)^2 - \frac{p^2}{\ell^2_p}\left(\frac{1}{1-i\Delta f/f'_p}\right) - \frac{q^2}{\ell^2_q}\left(\frac{1}{1-i\Delta f/f'_q}\right)\right] \tag{41}$$

† The use of this expression throughout constitutes the Delta layer approximation which is the basis of a set of simple propagation expressions for well defined scattering regions (see Appendix C).

where

$$\Delta f = f_2 - f_1 = \frac{c}{2\pi}(K_2 - K_1)$$

$$\ell_p = C_p^{-1/2}(z_t)$$

$$\ell_q = C_q^{-1/2}(z_t)$$

$$f'_p = \frac{K_2^2 c}{4\pi C_p(z_1) z_f}$$

$$f'_q = \frac{K_2^2 c}{4\pi C_q(z_1) z_f}$$

$$z_f = \frac{(z_t - z_1) z_1}{z_t}$$

ℓ_p, ℓ_q, f'_p, and f'_q have implicit dependence on f_2. In actual applications the system bandwidth is usually small compared to the carrier frequency, f_c. Thus the above parameters vary little over the bandwidth and f_2 as it appears everywhere in Equation 31, except in Δf, can be replaced by f_c. This is consistent with dropping the $1 - \eta$ terms earlier. With these assumptions, Equation 39 describes a statistical process that is stationary in both space and frequency.

The delta layer approximation is not always justified particularly when the scattering layer is thick and comparable with the other problem dimensions. Appendix D demonstrates that finite layer thickness can be compensated for by correcting f'_p and f'_q with a multiplication factor and by multiplying $G(z_t, p, q, \Delta f)$ by $\exp(iR'\Delta f)$ where R' is a constant independent of Δf. This term can be neglected because it results in a uniform time shift of the signal. These corrections apply for all cases ranging from the thin layer to the case where both the transmitter and receiver are buried in the structured layer. The success of the simple scaling of f'_p and f'_q demonstrates the generality of the form shown in Equation 41 assuming f'_p and f'_q are properly chosen.

Equation 41 can be specialized to two cases which bound the frequency selective effects. The first case, where $C_p = C_q$, assumes isotropy of the effects about the propagation line of sight. In this case only one coordinate can be relevant so q can be set to zero. Finally, the remaining spatial argument, p^2/ℓ_p^2, transforms to $\Delta t^2/\tau_o^2$ when the effective motion is considered. The result is

$$G_2(z_t,\Delta t,\Delta f) = \frac{1}{(1-i\Delta f/f_2')} \exp\left[-\frac{\sigma_{\phi R}^2}{2}\left(\frac{\Delta f}{f_c}\right)^2 - \frac{\Delta t^2}{\tau_o^2}\left(\frac{1}{1-i\Delta f/f_2'}\right)\right] \qquad (42)$$

where

$$f_2' = \left\{\frac{4\pi^2}{K^4 c^2}\int_0^{z_t}\frac{dz'}{z'^2}\int_0^{z'}\frac{dz}{z^2}\left[I_u^2(z) + I_v^2(z) + 2I_{uv}^2(z)\right]\right\}^{-1/2}$$

$\sigma_{\phi R}^2$ has been used to limit $G_2(z_t,\Delta t,\Delta f)$ to the Rayleigh portion of the signal. The redefinition of f_2' preserves σ_t which was defined in Equation 38.

The second case, where $C_p >> C_q$, assumes that there is signal variation in only one direction with respect to the propagation line of sight. Transforming the spatial dependence to time, we get

$$G_1(z_t,\Delta t,\Delta f) = \frac{1}{(1-i\Delta f/f_1')^{1/2}} \exp\left[-\frac{\sigma_{\phi R}^2}{2}\left(\frac{\Delta f}{f_c}\right)^2 - \frac{\Delta t^2}{\tau_o^2}\left(\frac{1}{1-i\Delta f/f_1'}\right)\right] \qquad (43)$$

where $f_1' = f_2'/\sqrt{2}$. The generalized power spectrum is the two dimensional Fourier transform of $G(z_t,\Delta t,\Delta f)$.

$$\Gamma(f,\tau) = \int_{-\infty}^{\infty} d(\Delta f) \int_{-\infty}^{\infty} d(\Delta t) G(z_t,\Delta t,\Delta f) e^{-i2\pi\Delta f\tau} e^{i2\pi f\Delta t} \qquad (44)$$

where

f = frequency coordinate

τ = time delay coordinate

Evaluating Equation 44 with Equations 42 and 43

$$\Gamma_2(f,\tau) = 2^{3/4}\pi^{1/2} f_2'\tau_o \left(\frac{f_c}{f_2'\sigma_{\phi R}}\right)^{1/2} e^{-(\pi\tau_o f)^2} e^{-\frac{1}{2}[(\pi\tau_o f)^2 - 2\pi f_2'\tau]^2 \left(\frac{f_c}{f_2'\sigma_{\phi R}}\right)^2}$$

$$F\left\{\frac{1}{2^{1/2}}\left(\frac{f_2'\sigma_{\phi R}}{f_c}\right)\left[1 + \left((\pi\tau_o f)^2 - 2\pi f_2'\tau\right)\left(\frac{f_c}{f_2'\sigma_{\phi R}}\right)^2\right]\right\} \qquad (45)$$

where

$$F(z) = \int_{-\infty}^{\infty} e^{-x^4 - 2zx^2} dx$$

$$\Gamma_1(f,\tau) = 2^{1/2}\pi\tau_o f_1' \left(\frac{f_c}{f_1'\sigma_{\phi R}}\right) e^{-(\pi\tau_o f)^2} e^{-\frac{1}{2}[(\pi\tau_o f)^2 - 2\pi f_1'\tau]^2 \left(\frac{f_c}{f_1'\sigma_{\phi R}}\right)^2} \qquad (46)$$

Both Γ_1 and Γ_2 are nondimensional and normalized to unity when integrated over all f and τ. When integrated over all τ, they reduce to Equation 33, the flat fading spectrum. Both functions depend on three nondimensional quantities: $\tau_o f$, $f'\tau$, and $f_c/(f'\sigma_{\phi R})$ which must be specified to define the generalized power spectra.

The generalized power spectra in Equations 45 and 46 represent a stationary process with a Rayleigh distributed amplitude. This constitutes a complete statistical description of the signal structure excluding mean and asymmetric bandwidth effects. Figures 2 through 8 show selected plots of the generalized power spectra. For $\sigma_{\phi R} f'/f_c$ large, the gaussian term in frequency dominates. For $\sigma_{\phi R} f'/f_c$ small, the energy arrives at higher frequencies for longer delays. This behavior is intuitively pleasing because increasing frequency corresponds to increasing energy angle of arrival with respect to the propagation line of sight which, in turn, implies longer delay because of longer geometric path lengths. For $\Gamma_2(f,\tau)$, some energy is at low frequency regardless of the delay because of energy scattering from regions out of the plane determined by the line of sight and the direction of the effective velocity. The most significant difference between $\Gamma_1(f,\tau)$ and $\Gamma_2(f,\tau)$ is in the total energy arriving at any delay as shown in Figures 9-12. $\Gamma_2(f,\tau)$ is usually the more serious threat because it leads to more delay.

The effects of a disturbed linear channel can be expressed in terms of the channel impulse response function, $h(t,\tau)$. The received signal modulation is

$$S_r(t) = \int_{-\infty}^{\infty} h(t,\tau) S_t(t-\tau)\, d\tau \qquad (47)$$

where $S_t(t)$ is the transmitted modulation. The impulse response function is

$$h(t,\tau) = \int_{-\infty}^{\infty} U(z_t,t,f)\, e^{iK \int_0^{z_t} \overline{n_i}\, dz} \; e^{i2\pi(f-f_c)\tau}\, df \qquad (48)$$

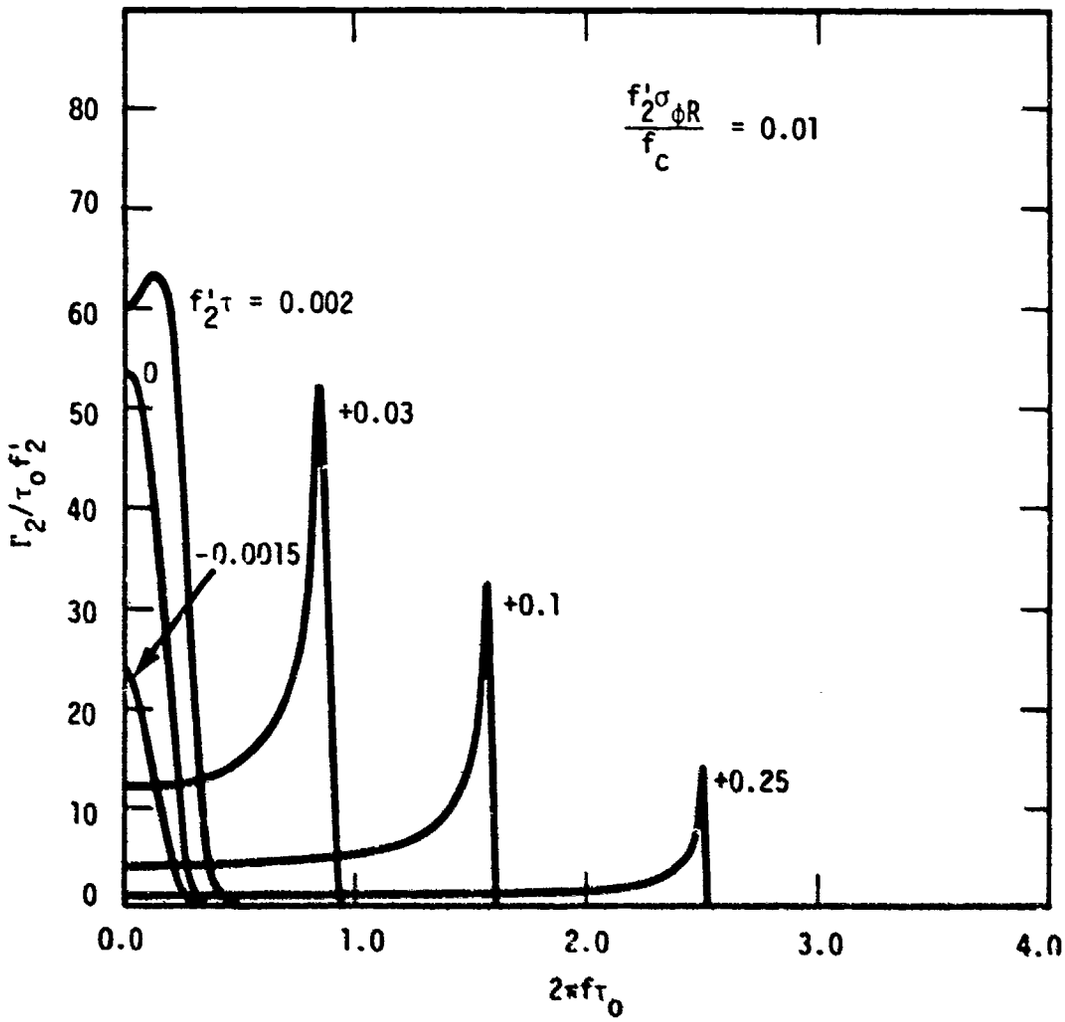

Figure 2. Two-dimensional generalized power spectrum.

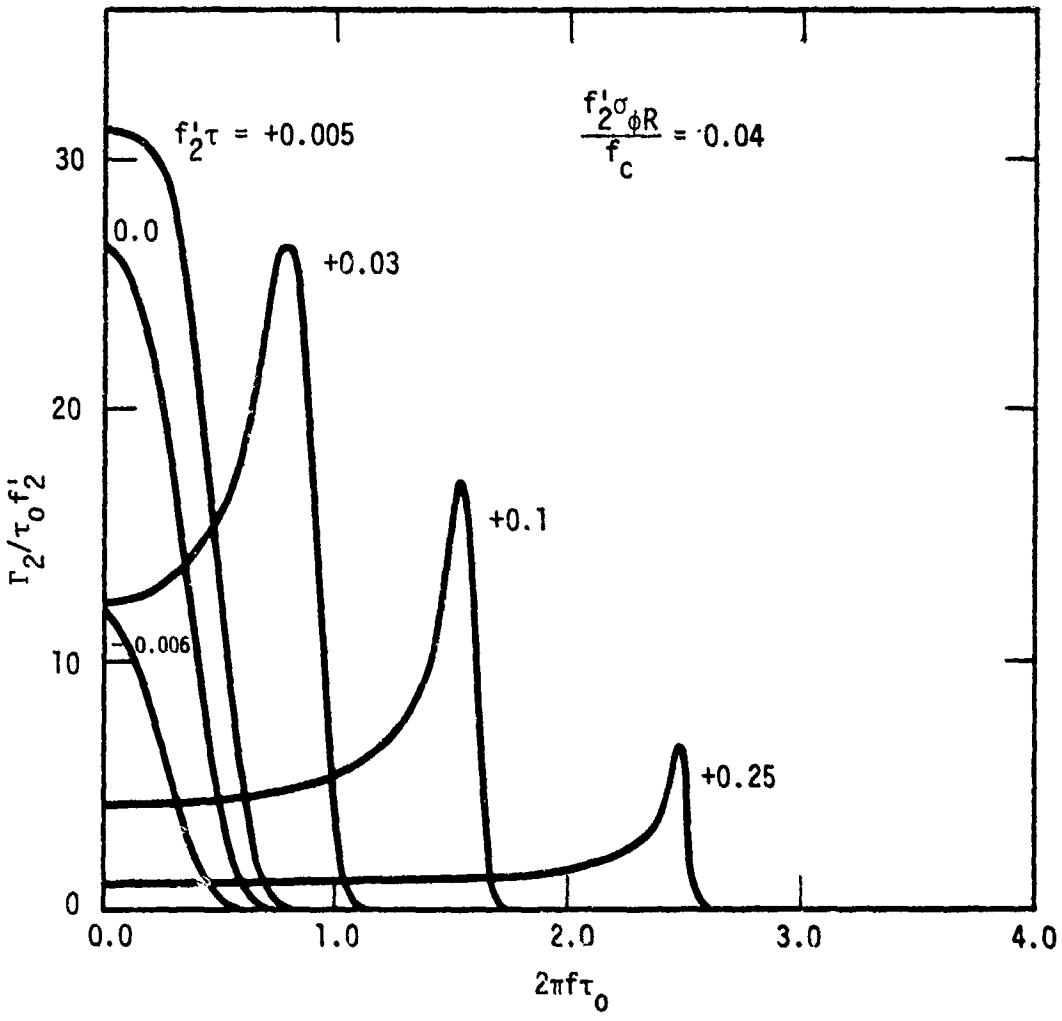

Figure 3. Two-dimensional generalized power spectrum.

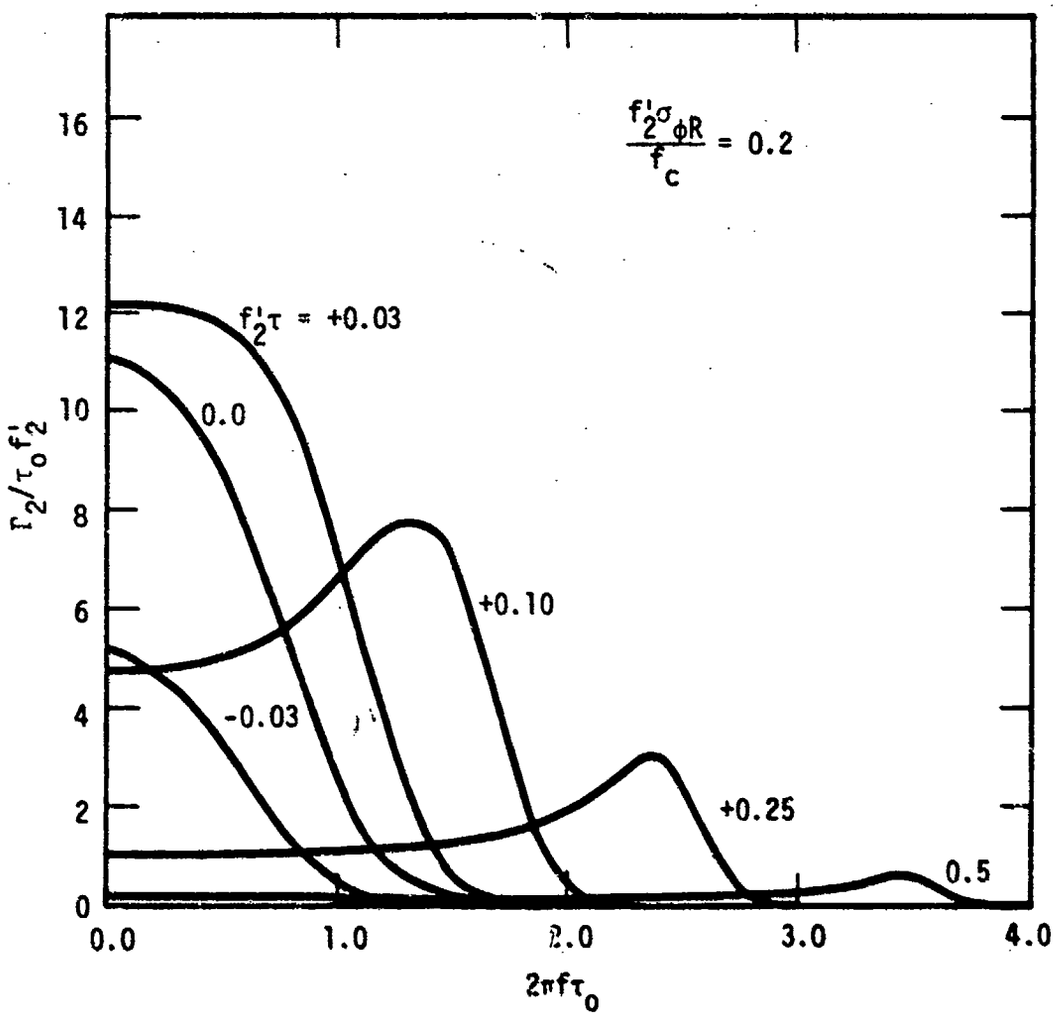

Figure 4. Two-dimensional generalized power spectrum.

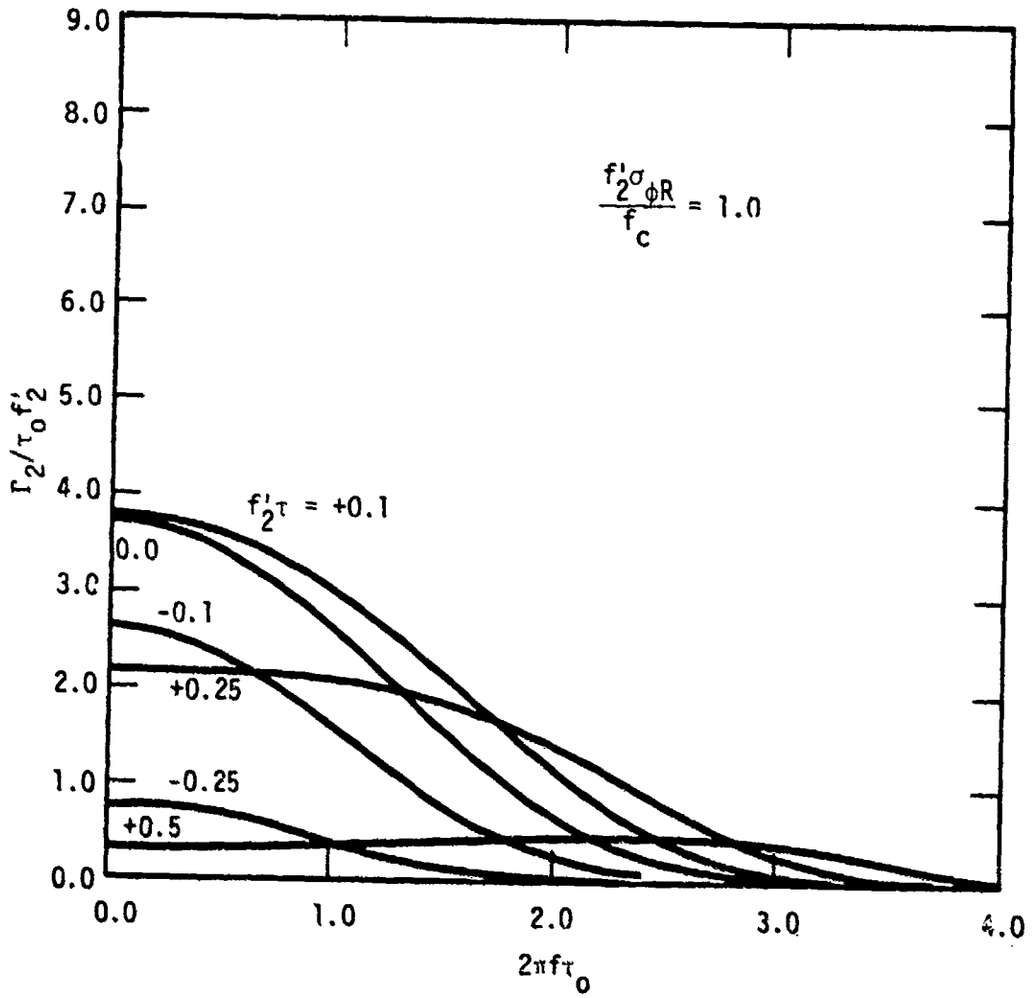

Figure 5. Two-dimensional generalized power spectrum.

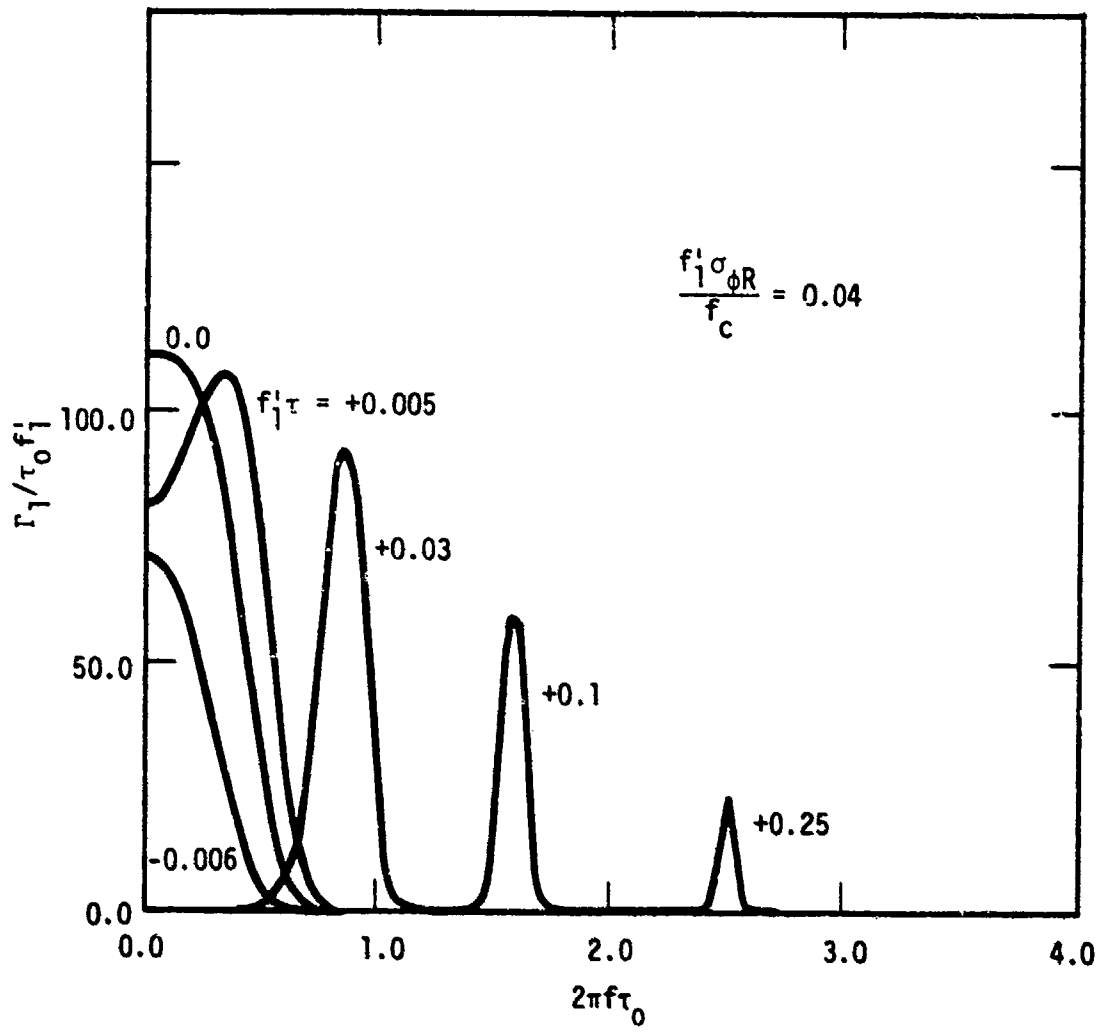

Figure 6. One-dimensional qeneralized power spectrum.

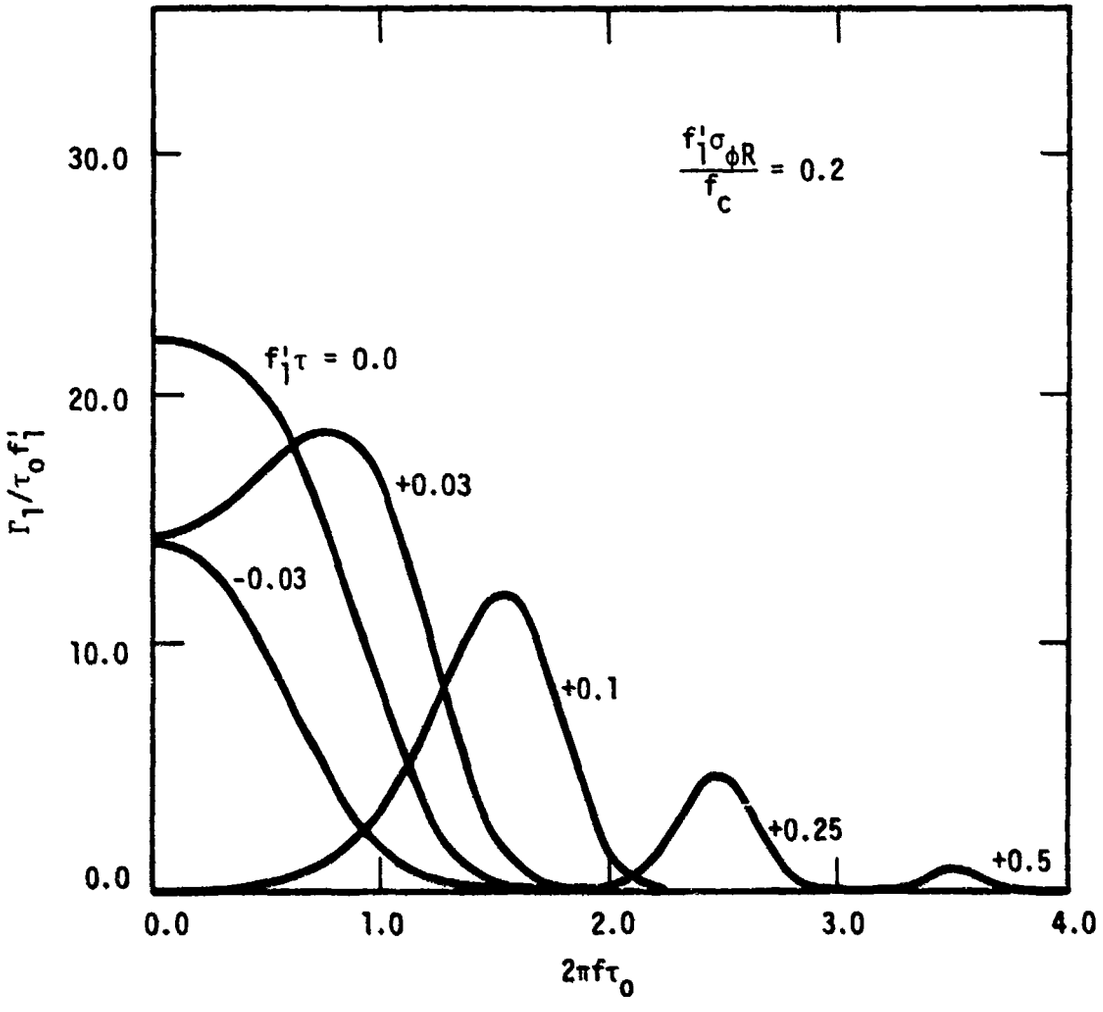

Figure 7. One-dimensional generalized power spectrum.

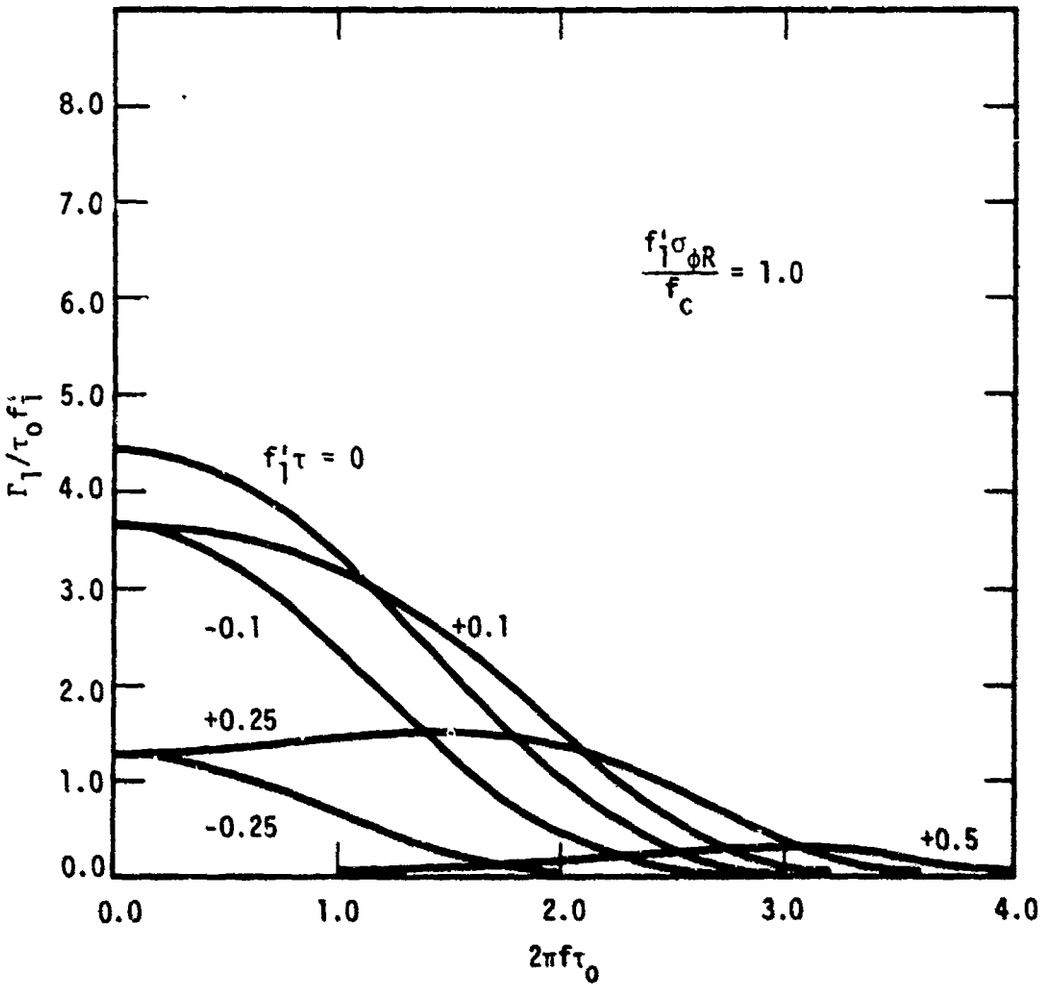

Figure 8. One-dimensional generalized power spectrum.

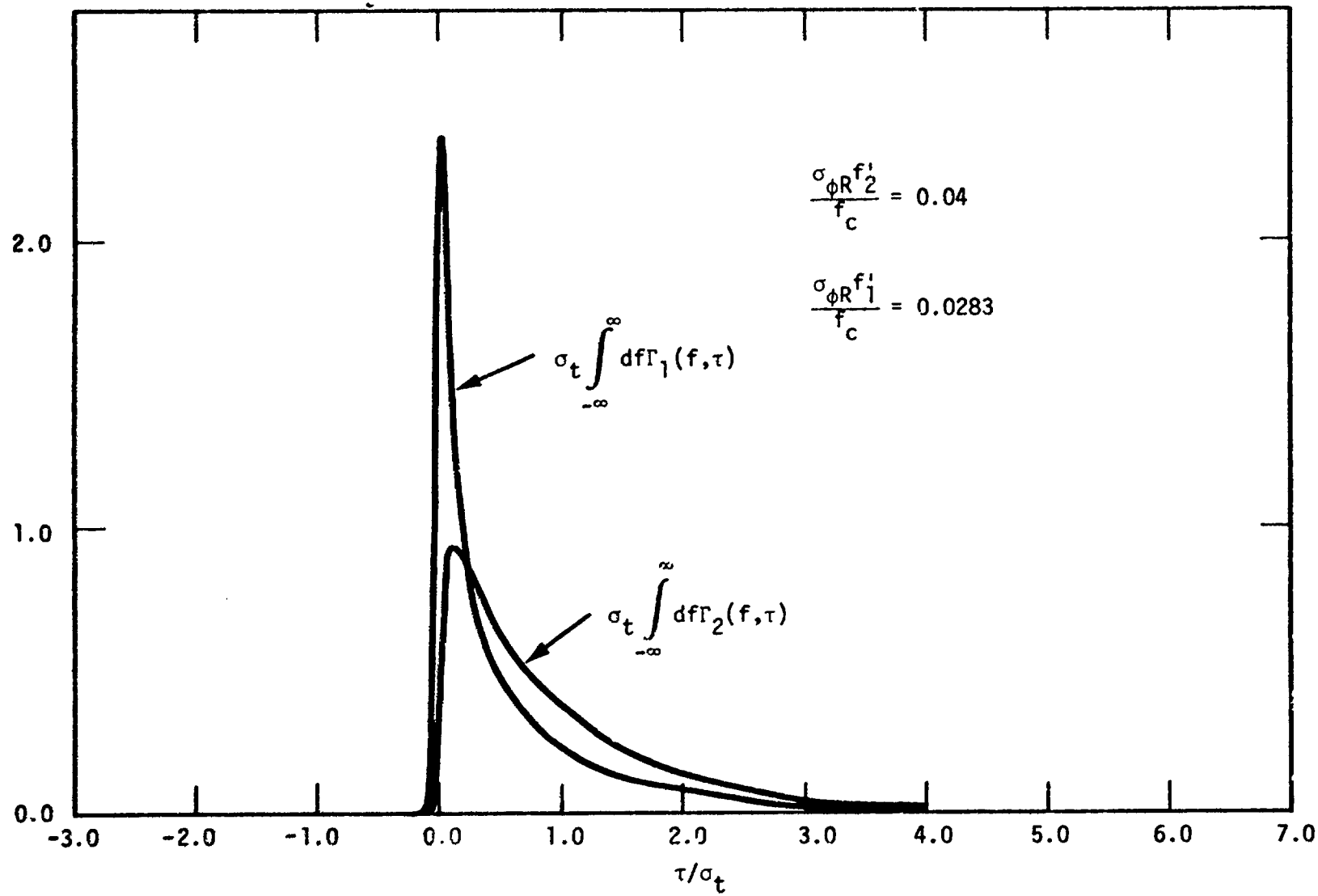

Figure 9. Energy arrival as a function of delay.

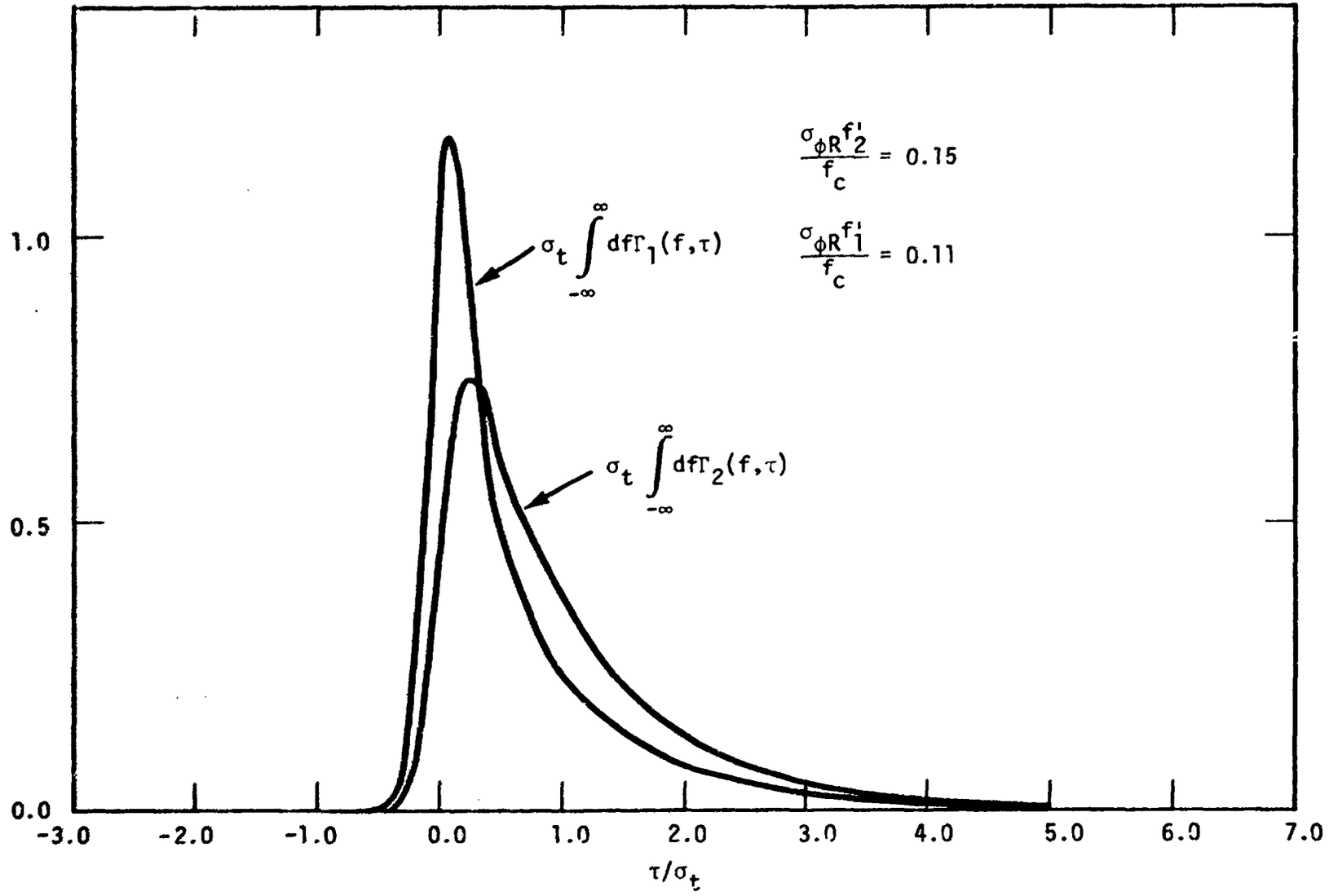

Figure 10. Energy arrival as a function of delay.

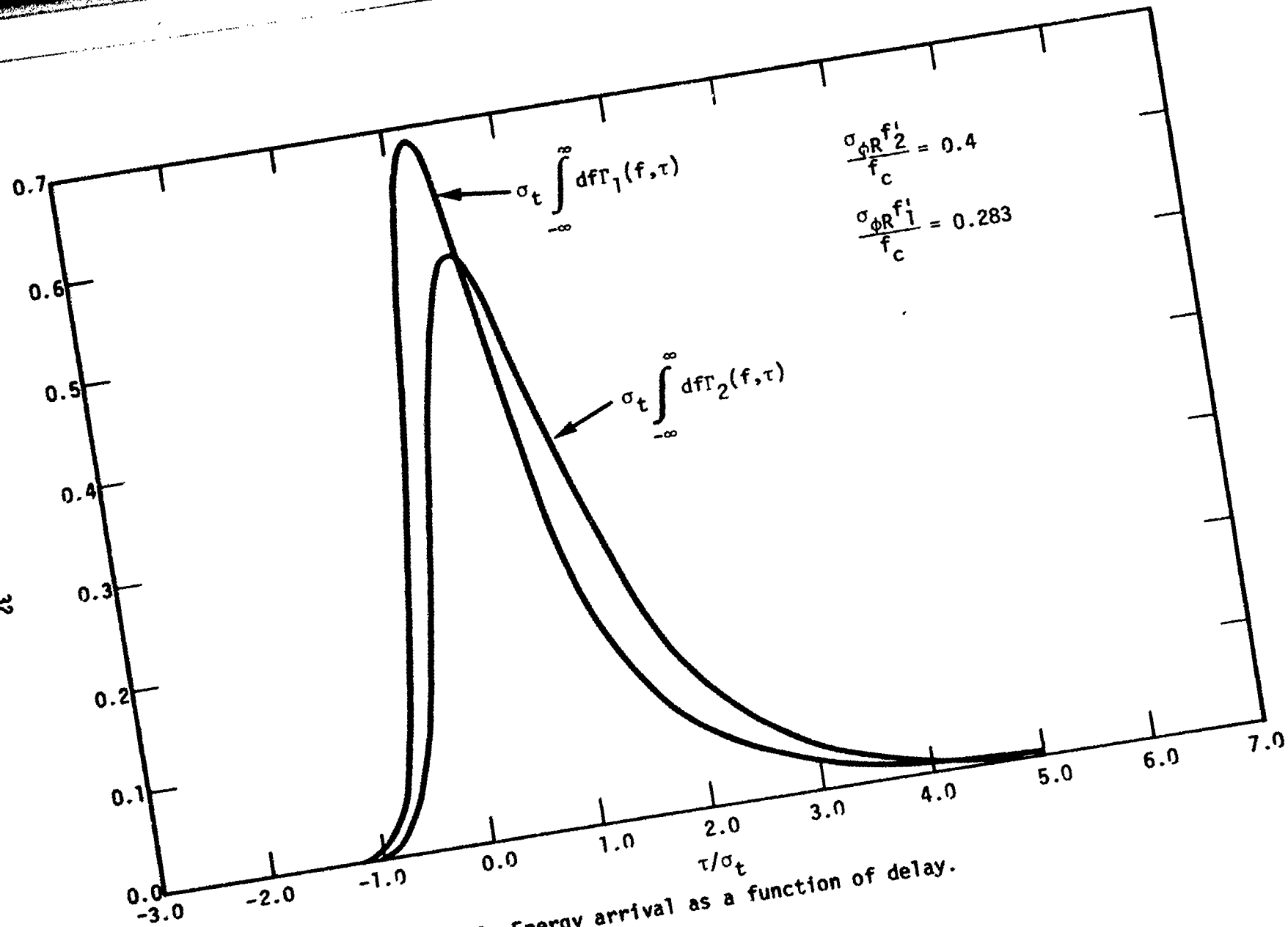

Figure 11. Energy arrival as a function of delay.

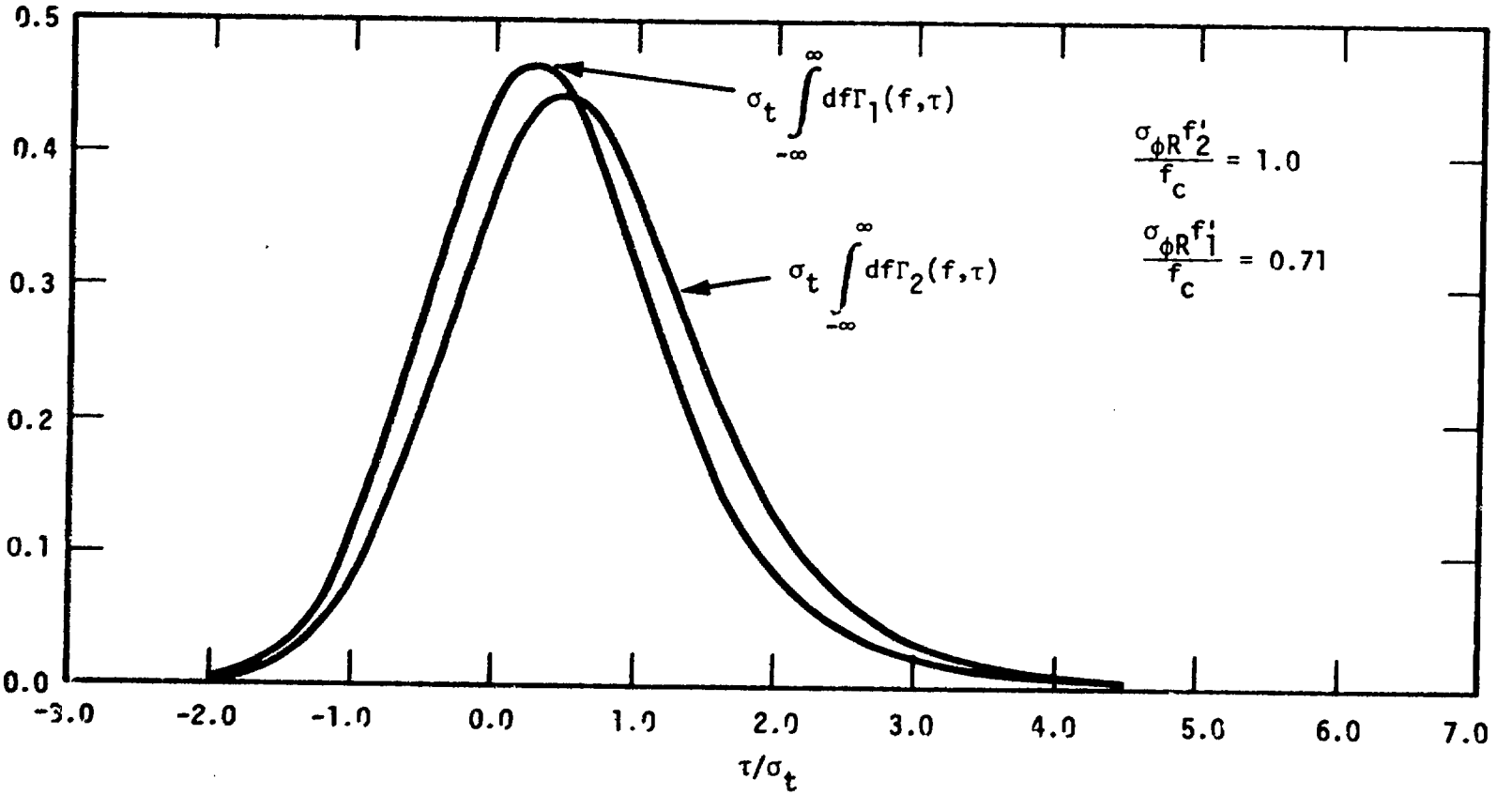

Figure 12. Energy arrival as a function of delay.

where $\overline{n_i}$ is the mean index of refraction. $U(z_t,t,f)$ is the carrier signal defined in Equation 15 but expressed as a function of time as perceived at the receiver. The mean index of refraction can be expanded about the carrier frequency resulting in the following form for the channel impulse response function.

$$h(t,\tau) = e^{i\frac{2\pi f_c}{c}z_t} e^{-i\frac{cr_o TEC}{f_c}} \int df\, U(z_t,t,f) e^{-i\frac{cr_o TEC(f-f_c)^2}{f_c^3}} e^{-i2\pi f\left(\tau - \frac{z_t}{c} - \frac{cr_o TEC}{2\pi f_c^2}\right)} \tag{49}$$

where TEC is the total electron content, r_o is the classical electron radius, and only terms through $(f-f_c)^2$ have been retained. Equation 49 is a rather complete description including doppler effects from changes in z_t and the most important TEC effects: phase shifting, group delay, and dispersion. Let the scintillation impulse response function be defined by

$$h_s(t,\tau) = \int df\, U(z_t,t,f) e^{-i2\pi f\tau} \tag{50}$$

Since $U(z_t,t,f)$ is Rayleigh distributed, then so is $h_s(t,\tau)$. With some manipulation, it can be shown that the frequency power spectrum of $h_s(t,\tau)$ is either Equation 45 or 46. Thus Equation 45 or 46 provides a complete statistical description of the scintillation impulse response function. The mean value of τ in Equation 50 is

$$\overline{\tau_2} = \frac{1}{2\pi f_2'} \qquad \text{or} \tag{51a}$$

$$\overline{\tau_1} = \frac{1}{4\pi f_1'} \tag{51b}$$

depending on which of the two generalized power spectra is used.

Equations 45 or 46, 49, and 50 permit the sampling of the channel impulse response function. First, using methods described in Appendix E, samples of $h_s(t,\tau)$ are generated. For the general case, $h_s(t,\tau)$ is next Fourier transformed with respect to τ, multiplied by the dispersion and time delay terms, inverse transformed with respect to f, and finally multiplied by the doppler and TEC phase term. In most cases scintillation effects are evaluated separately from the other effects and the scintillation impulse response function is used as the channel impulse response function. If the scintillation delay is small with respect to the modulation symbol, then the delay can be ignored. Then Equations 45 and 46 can be replaced by Equations 33 or 34. The scintillation impulse response function is only a function of time. Thus,

$$h(t,\tau) = e^{i\frac{2\pi f_c}{c} z_t} e^{-\frac{icr_o TEC}{f_c}} h_s(t)\, e^{-i\pi/4} \left(\frac{\pi f_c^3}{cr_o TEC}\right)^{1/2} e^{i\frac{\pi^2 f_c^3}{cr_o TEC}\left(\tau - \frac{z_t}{c} - \frac{cr_o TEC}{2\pi f_c^2}\right)^2} \qquad (52)$$

This completes the discussion of the generalized power spectrum and its value in providing a complete statistical description of a scintillated signal. Most important, methods were presented to economically generate disturbed signals for test and evaluation applications.

5. SUMMARY

The preceding sections have developed a sequence of models and algorithms that specify the index of refraction fluctuation environments, calculate various signal structure statistical parameters, and lastly, permit the sampling of the channel impulse response function consistent with the signal structure statistical parameters. The geometric aspects of the

problem were treated in all generality using a locally homogeneous approximation. All of the preceding development applies to $2 \leq n < 3$. This range includes the presently held value for strongly structured ionospheric environments. We usually assumed $\sigma_\phi^2 >> 1$, but this restriction is not very serious. It can be neglected without seriously impacting any results as they may impact communication or radar systems.

REFERENCES

1. Wittwer, L. A., UHF Propagation Effects in Scintillated Environments, AFWL-TR-76-304, Air Force Weapons Laboratory, Kirtland AFB, NM, August 1977.

2. Wittwer, L. A., The Propagation of Satellite Signals Through Turbulent Media, AFWL-TR-77-183, Air Force Weapons Laboratory, Kirtland AFB, NM, January 1978.

3. Phelps, A. D. R., and Sagalyn, R. C., "Plasma Density Irregularities in the High-Latitude Top Side Ionosphere," J. Geophys. Res., Vol. 81, No. 4, February 1976.

4. Dyson, P. L., McClure, J.P., and Hanson W. B., "In Situ Measurements of the Spectral Characteristics of F Region Ionospheric Irregularities," J. Geophys. Res., Vol. 79, April, 1974.

5. Morse, F. A., et al., "EQUION, An Equatorial Ionospheric Irregularity Experiment," J. Geophys. Res., Vol. 82, 578, 1977.

6. Baker, K. D., et al., Electron Density Structure in Barium Clouds – Measurements and Interpretation, DNA 4561F, Utah State University, February 1978.

7. Pongratz, M., and Fitzgerald T., Temporal Variations of the Ave Fria Dos Striation Power Spectral Density, Private Communication, Los Alamos Scientific Laboratory, July 1979.

8. Baker, K. D., Rocket Measurements of Auroral Electron Density Irregularities in Support of the Defense Nuclear Agency Wideband Satellite, DNA 4676T, Utah State University, August 1978.

9. Ossakow, S. L., A Review of Recent Results on Spread F Theory, NRL Memorandum Report 3909, Naval Research Laboratory, January 1979.

10. Tatarski, V. I., Wave Propagation in a Turbulent Medium, Dover Publications, Inc., New York 1961.

11. Yeh, K. C., and Liu, C. H., "An Investigation of Temporal Moments of Stochastic Waves," Radio Science, Vol. 12, Sept.-Oct. 1977.

APPENDIX A
DERIVATION OF THE LINEAR INTEGRATED PHASE SPECTRUM

Let the integrated phase be written as

$$\phi(\bar{r}) = K\int \Delta n_i(\bar{r},z)dz \tag{A-1}$$

where

z = coordinate along the propagation line of sight (LOS)

$\bar{r}$ = coordinate vector in perpendicular to the LOS

Δn_i = index of refraction fluctuation

K = wave number of carrier signal

Now look at a portion of the integral in Equation A-1.

$$\Delta\phi(\bar{r}_1,z_1) = K\int_{z_1}^{z_1+\Delta z} \Delta n_i(\bar{r}_1,z)dz \tag{A-2}$$

The correlation function for $\Delta\phi$ is

$$R_{\Delta\phi}(\bar{\rho},\varepsilon) = K^2\int_{z_1}^{z_1+\Delta z} dz \int_{z_2}^{z_2+\Delta z} dz' \overline{\Delta n_i(\bar{r}_1,z)\Delta n_i(\bar{r}_2,z')} \tag{A-3}$$

$$= K^2\Delta z\int_{-\Delta z}^{\Delta z} d\eta R(\bar{\rho},\eta-\varepsilon)(1-|\eta|/\Delta z) \tag{A-4}$$

where

$$\bar{\rho} = \bar{r}_1 - \bar{r}_2$$

$$\varepsilon = z_1 - z_2$$

$$R(\bar{\rho}, z-z') = \overline{\Delta n_i(\bar{r}_1, z)\Delta n_i(\bar{r}_2, z')}$$

If we assume that $R(\bar{\rho}, z-z')$ has a decorrelation distance L_z for the second argument, then it is clear that, as Δz becomes larger than L_z, $R_{\Delta\phi}$ is significant only for small ε. As Δz increases, the contributions to the total phase correlation function from each layer of thickness Δz become uncorrelated. Thus for Δz larger than L_z and assuming that the statistical parameters in R do not vary greatly over Δz, we can write the phase correlation function as

$$R_\phi(\bar{\rho}) = K^2 \int dz \int_{-\infty}^{\infty} d\varepsilon \; R_{\Delta\phi}(\bar{\rho}, \varepsilon) \tag{A-5}$$

where $R_{\Delta\phi}$ depends on z through its statistical parameters. Equation A-5 allows us to define the differential linear phase spectrum. Let

$$P_\phi(\bar{K}_\rho) = \int_{-\infty}^{\infty} d^2\bar{\rho} \; e^{i\bar{K}_\rho \cdot \bar{\rho}} \int dz \int_{-\infty}^{\infty} d\varepsilon \; K^2 R_{\Delta\phi}(\bar{\rho}, \varepsilon) \tag{A-6}$$

Since we have assumed that $R_{\Delta\phi}(\bar{\rho}, \varepsilon)$ changes slowly over Δz and hence L_z, the integral over z can be taken to the outside and differentiated. The result is the differential linear phase spectrum.

$$\frac{dP_\phi(\bar{K}_\rho)}{dz} = \int_{-\infty}^{\infty} d^2\bar{\rho} \; e^{i\bar{K}_\rho \cdot \bar{\rho}} \int_{-\infty}^{\infty} d\varepsilon \; K^2 R_{\Delta\phi}(\bar{\rho}, \varepsilon) \tag{A-7}$$

The operations in A-7 are equivalent to multiplying the in situ index of refraction spectrum by K^2 and setting the wavenumber along the LOS equal to zero. Thus for a generalized power law spectrum

$$\frac{dP_\phi(K_x,K_y)}{dz} = \frac{8\pi^{3/2}K^2\overline{\Delta n_i^2}L_xL_yL_z\Gamma(n)}{\Gamma(n-3/2)(1+L_x^2K_x^2+L_y^2K_y^2)^n} \tag{A-8}$$

In the derivation of Equation A-8 it was assumed that L_z was smaller than Δz and hence the scattering layer thickness. If L_z becomes comparable to or larger than z_s, the layer thickness, then the earlier derivation fails. Let

$$\phi(\bar{r}) = \left(\frac{2}{\pi}\right)^{1/4} K\int_{-\infty}^{\infty}\Delta n_i(\bar{r},z)e^{-(z/z_s)^2}\,dz \tag{A-9}$$

where the exponential represents a finite scattering layer along the LOS. Δn_i is for present purposes taken as a homogeneous stationary process. After some manipulation

$$R_\phi(\bar{\rho}) = K^2z_s\int_{-\infty}^{\infty}R(\bar{\rho},\varepsilon)e^{-\varepsilon^2/2z_s^2}\,d\varepsilon \tag{A-10}$$

where global homogeneity has been assumed. The phase power spectrum is

$$P_\phi(K_x,K_y) = \frac{1}{2\pi}\int_{-\infty}^{\infty}\frac{8\pi^{3/2}K^2\overline{\Delta n_i^2}L_xL_yL_z\Gamma(n)z_s^2}{(1+K_x^2L_x^2+K_y^2L_y^2+K_\varepsilon^2L_z^2)^n\Gamma(n-3/2)}(2\pi)^{1/2}e^{-\frac{1}{2}\left[K_\varepsilon L_z\left(\frac{z_s}{L_z}\right)\right]^2}dK_\varepsilon \tag{A-11}$$

If z_s/L_z is large, then the exponential integrates out.

$$P(K_x,K_y) \approx \frac{8\pi^{3/2}\overline{\Delta n_i^2}K^2 L_x L_y L_z z_s \Gamma(n)}{(1+K_x^2L_x^2+K_y^2L_y^2)^n \Gamma(n-3/2)} \qquad \text{(A-12)}$$

Equation A-12 is Equation A-8 integrated over z. Now if z_s/L_z is small, the spectrum has two regimes. For $K_x^2L_x^2 + K_y^2L_y^2 > L_z^2/z_s^2$, Equation A-12 still holds since the exponential dominates the integral. For $K_x^2L_x^2 + K_y^2L_y^2 < L_z^2/z_s^2$, the power law dependence on K_ε dominates and

$$P(K_x,K_y) \approx \frac{2(2\pi)^{3/2}K^2\overline{\Delta n_i^2}L_x L_y z_s^2 \Gamma(n-1/2)}{(1+K_x^2L_x^2+K_y^2L_y^2)^{n-1/2}\Gamma(n-3/2)} \qquad \text{(A-13)}$$

Thus, the actual phase spectrum has two distinct parts. The low frequency part is one power shallower in slope and goes as the square of the layer thickness.

In general, the spectrum in A-12 is most accurate as, with one exception, L_z doesn't get appreciably larger than z_s. For these cases the use of A-13 would be a gross overestimate of the effects. The one possible exception is when the LOS is nearly parallel to the magnetic field in the ionospheric scintillation case. In this case the outer scale along the magnetic field may be very long compared to the thickness of the region with any scattering strength. Even in this case, Equation A-12 will not underestimate the effects and gives the best representation for the larger transverse wave numbers.

APPENDIX B

CALCULATION OF THE MEAN SQUARE LOG AMPLITUDE FLUCTUATION AND THE RAYLEIGH PHASE VARIANCE

The equation for the mean square log amplitude fluctuation is

$$\overline{\chi^2} = \int_0^{z_t} dz \int_{-\infty}^{\infty} \frac{dK_x}{2\pi} \int_{-\infty}^{\infty} \frac{dK_y}{2\pi} \sin^2\left[\frac{(K_x^2+K_y^2)(z_t-z)z}{2Kz_t}\right] \frac{dP_\phi(K_x,K_y)}{dz} \qquad \text{(B-1)}$$

where

$$\frac{dP_\phi(K_x,K_y)}{dz} = \frac{d\sigma_\phi^2}{dz} \frac{4\pi(L_x^2L_y^2-L_{xy}^2)^{1/2}(n-1)}{(1+L_x^2K_x^2+L_y^2K_y^2+2L_{xy}K_xK_y)^n} \qquad \text{(B-2)}$$

Equation B-1 using B-2 is not integrable but two useful limits can be evaluated depending on the size of M(z) where

$$M(z) = \frac{(L_x^2+L_y^2)(z_t-z)z}{Kz_t(L_x^2L_y^2-L_{xy}^2)} \qquad \text{(B-3)}$$

First, let us look at large M(z). We expand

$$\sin^2\left[\frac{(K_x^2+K_y^2)(z_t-z)z}{2Kz_t}\right] = \frac{1}{2} - \frac{1}{2}\cos\left[\frac{(K_x^2+K_y^2)(z_t-z)z}{Kz_t}\right] \qquad \text{(B-4)}$$

and examine the integral contribution from the second term on the right side of the equation. If L_x and L_y are of comparable magnitude, then the integral is dominated by values of K_x and K_y where $L_x^2K_x^2 + L_y^2K_y^2 + 2L_{xy}K_xK_y < 1$. The resulting integral is then proportional to $M(z)^{-1}$. If L_x and L_y are

significantly different in size, then the integral is proportional to $M(z)^{-1/2}$. Thus the second term on the right in Equation B-4 does not contribute to $\overline{\chi^2}$ when $M(z)$ is large. For $M(z)$ large

$$\overline{\chi^2} \approx \frac{1}{2}\int_0^{z_t} \frac{d\sigma_\phi^2}{dz}\, dz \tag{B-5}$$

For $M(z)$ small, the $\overline{\chi^2}$ integral is dominated by values of K_x and K_y where $L_x^2K_x^2+L_y^2K_y^2+2L_{xy}K_xK_y \gg 1$. Then

$$\overline{\chi^2} \approx \int_0^{z_t} dz \int_{-\infty}^{\infty} \frac{dK_x}{2\pi} \int_{-\infty}^{\infty} \frac{dK_y}{2\pi} \sin^2\left[\frac{(K_x^2+K_y^2)(z_t-z)z}{2Kz_t}\right] \frac{d\sigma_\phi^2}{dz} \frac{4\pi(L_x^2L_y^2-L_{xy}^2)^{1/2}(n-1)}{(L_x^2K_x^2+L_y^2K_y^2+2L_{xy}K_xK_y)^n} \tag{B-6}$$

First, we rotate in K_x-K_y space to eliminate the K_xK_y term.

$$\overline{\chi^2} = \int_0^{z_t} dz \int_{-\infty}^{\infty} \frac{dK_1}{2\pi} \int_{-\infty}^{\infty} \frac{dK_2}{2\pi} \sin^2\left[\frac{(K_1^2+K_2^2)(z_t-z)z}{2Kz_t}\right] \frac{d\sigma_\phi^2}{dz} \frac{4\pi(L_x^2L_y^2-L_{xy}^2)^{1/2}(n-1)}{(L_1^2K_1^2+L_2^2K_2^2)^n} \tag{B-7}$$

where

$$L_1^2 = \frac{1}{2}\left[L_x^2+L_y^2-((L_x^2-L_y^2)^2+4L_{xy}^2)^{1/2}\right]$$

$$L_2^2 = \frac{1}{2}\left[L_x^2+L_y^2+((L_x^2-L_y^2)^2+4L_{xy}^2)^{1/2}\right]$$

Let

$$K_1 = \kappa\cos\theta$$

$$K_2 = \kappa\sin\theta$$

$$a^2 = \kappa^2 \frac{(z_t - z)z}{2Kz_t}$$

Now

$$\overline{\chi^2} = \int_0^{z_t} dz \left[\frac{(n-1)}{2^{n-1}\pi}\int_0^{\infty} \frac{\sin^2(a^2)}{a^{2n-1}}\, da\right]\left[\frac{(z_t-z)z}{Kz_t}\right]^{n-1} \frac{d\sigma_\phi^2}{dz}\left[\int_0^{2\pi} \frac{(L_x^2L_y^2-L_{xy}^2)^{1/2}\, d\theta}{(L_1^2\cos^2\theta+L_2^2\sin^2\theta)^n}\right] \tag{B-8}$$

The first bracket is approximately equal to $(n-1)/8$. The last bracket is approximately

$$\int_0^{2\pi} \frac{(L_x^2L_y^2-L_{xy}^2)^{1/2}d\theta}{(L_1^2\cos^2\theta+L_2^2\sin^2\theta)^n} \approx \frac{2\pi}{2^{n-1}}\left(\frac{L_x^2+L_y^2}{L_x^2L_y^2-L_{xy}^2}\right)^{n-1} \tag{B-9}$$

The final expression for $\overline{\chi^2}$ with small $M(z)$ is

$$\overline{\chi^2} \approx \frac{1}{2}\int_0^{z_t} dz M(z)^{n-1} g(n) \frac{d\sigma_\phi^2}{dz} \tag{B-10}$$

where $g(n)$ equals 0.68, 0.79, and 0.83 for values of n of 1.75, 2.0, and 2.5 respectively. For simplicity we will let $g(n)$ be unity. The error incurred is small particularly for n equal or greater than two which is the most common case.

This last case can be combined with Equation B-5 to get the final result.

$$\overline{\chi^2} = \frac{1}{2}\int_0^{z_t} \frac{d\sigma_\phi^2}{dz}\left(\frac{M(z)}{1+M(z)}\right)^{n-1} dz \tag{B-11}$$

Comparison with explicit propagation calculations has shown Equation B-11 to be accurate to about twenty five percent everywhere and within ten percent if $M(z)$ is small over the entire integral.

For small $M(z)$, the phase variance is divisible into the Rayleigh phase variance and the remainder. The Rayleigh phase variance is defined by

$$\sigma^2_{\phi R} \equiv \frac{(n-1)}{4^{n-2}} \int_{a_c}^{\infty} \frac{da}{a^{2n-1}} \int_{0}^{z_t} \frac{dz}{2} \frac{d\sigma^2_\phi}{dz} M(z)^{n-1} \tag{B-12}$$

where the notation of Equation B-8 has been used. a_c is chosen by using Equation B-8 to determine that portion of the integral over a that contributes negligibly to $\overline{\chi^2}$.

$$\frac{(n-1)}{4^{n-2}} \int_{0}^{a_c} \frac{\sin^2(a^2)}{a^{2n-1}} da \int_{0}^{z_t} \frac{dz}{2} \frac{d\sigma^2_\phi}{dz} M(z)^{n-1} = \overline{\chi^2_c} \tag{B-13}$$

Equation B-13 can be simplified using Equation B-11 and setting

$$\sin^2(a^2) \approx a^4$$

Integrating over a, remembering that $M(z)$ is small

$$\frac{a_c^{6-2n}}{6-2n} = \overline{\chi^2_c} \left[\frac{(n-1)}{4^{n-2}} \overline{\chi^2} \right]^{-1} \tag{B-14}$$

Similarly with Equation B-12

$$\sigma^2_{\phi R} = \frac{1}{(2n-2)a_c^{2n-2}} \left[\frac{(n-1)}{4^{n-2}} \overline{\chi^2} \right] \tag{B-15}$$

Combining Equations B-14 and B-15

$$\sigma_{\phi R}^2 = \frac{\left[(6-2n)\overline{\chi_c^2}\right]^{\frac{n-1}{n-3}}}{2n-2} \left(\frac{(n-1)}{2^{n-2}\pi}\overline{\chi^2}\right)^{\frac{2}{3-n}} \qquad \text{(B-16)}$$

The restriction to small M(z) can be lifted by limiting $\sigma_{\phi R}^2$ to σ_ϕ^2.

$$\sigma_{\phi R}^2 = \text{minimum}\left\{\sigma_\phi^2, \frac{\left[(6-2n)\overline{\chi_c^2}\right]^{\frac{n-1}{n-3}}}{2n-2}\left(\frac{(n-1)}{4^{n-2}}\overline{\chi^2}\right)^{\frac{2}{3-n}}\right\} \qquad \text{(B-17)}$$

If $\overline{\chi_c^2}$ equals 1.0×10^{-1} and n = 2,

$$\sigma_{\phi R}^2 = \text{minimum}(\sigma_\phi^2, 2.5\overline{\chi^2}^2) \qquad \text{(B-18)}$$

This quantity will be used when reconstructing Rayleigh signal structures.

APPENDIX C
THE DELTA LAYER APPROXIMATION

This approximation consists of using

$$\frac{d\sigma_\phi^2}{dz} = \sigma_\phi^2 \delta(z-z_1) \tag{C-1}$$

where

$$\sigma_\phi^2 = \int_0^{z_t} L_z \frac{2\pi^{1/2}\Gamma(n-1)}{\Gamma(n-3/2)} K^2 \overline{\Delta n_i^2}\, dz$$

$$L_z = \frac{L_r L_s L_t}{(L_x^2 L_y^2 - L_{xy})^{1/2}} \quad \text{evaluated at} \quad z$$

and z_1 marks the structured layer. In the following all of the scale sizes used are evaluated at z_1.

The mean square log amplitude fluctuation is

$$\overline{x^2} = \frac{\sigma_\phi^2}{2}\left[\frac{M(z_1)}{1+M(z_1)}\right]^{n-1} \tag{C-2}$$

where

$$M(z_1) = \frac{(L_x^2+L_y^2)z_f}{K(L_x^2 L_y^2 - L_{xy}^2)}$$

$$z_f = \frac{(z_t - z_1)z_1}{z_t}$$

The perpendicular decorrelation time is

$$\tau_1 = B(n,\sigma_\phi^2)\left[B_n\sigma_\phi^2\left(\left(\frac{z_1}{z_t}\right)^2 \frac{L_y^2V_x^2+L_x^2V_y^2-2L_{xy}V_xV_y}{L_x^2L_y^2-L_{xy}^2}\right)^{m/2}\right]^{-1/m} \qquad \text{(C-3)}$$

where

$$V_x = \overline{V} \cdot \hat{x}$$

$$V_y = \overline{V} \cdot \hat{y}$$

$$\overline{V} = \left(\frac{z_1-z_t}{z_1}\right)\overline{V}_{tr} + \frac{z_t}{z_1}\overline{V}_{st} - \overline{V}_{re}$$

Let

$$\tan(2\varepsilon) = \frac{2L_{xy}}{L_x^2 - L_y^2}$$

$$p = x\cos\varepsilon - y\sin\varepsilon$$

$$q = x\sin\varepsilon + y\cos\varepsilon$$

$$C_p = \frac{\sigma_\phi^2 B_n}{2}\left(\frac{z_1}{z_t}\right)^2[L_x^2+L_y^2+((L_x^2-L_y^2)^2+4L_{xy}^2)^{1/2}]/(L_x^2L_y^2-L_{xy}^2)$$

$$C_q = \frac{\sigma_\phi^2 B_n}{2}\left(\frac{z_1}{z_t}\right)^2[L_x^2+L_y^2-((L_x^2-L_y^2)^2+4L_{xy}^2)^{1/2}]/(L_x^2L_y^2-L_{xy}^2)$$

The parallel and total signal decorrelation times are

$$\tau_{\parallel} = \frac{3.7K}{(C_p^{2/3}+C_q^{2/3})^{3/2}\,|(\overline{V}_{re}-\overline{V}_{st}) \cdot \hat{z}|} \qquad \text{(C-4)}$$

$$\tau_o = \text{minimum}\,(\tau_1, \tau_{\parallel}) \qquad \text{(C-5)}$$

The signal angle of arrival distribution is in the p-q system

$$P_\theta(\theta_p,\theta_q) = \frac{K^2}{4\pi(C_qC_p)^{1/2}}\, e^{-\frac{K^2}{4}\left(\frac{\theta_p^2}{C_p}+\frac{\theta_q^2}{C_q}\right)} \qquad \text{(C-6)}$$

The variance of the energy arrival time is

$$\sigma_t^2 = \frac{\sigma_{\phi R}^2}{K^2 c^2} + \frac{2\sigma_\phi^4 B_n^2 z_f^2}{K^4 c^2} \frac{(L_x^4 + L_y^4 + 2L_{xy}^2)}{(L_x^2 L_y^2 - L_{xy}^2)^2} \tag{C-7}$$

and the frequency selective bandwidth is

$$f_o = (2\pi\sigma_t)^{-1} \tag{C-8}$$

Finally

$$f_1' = \frac{F}{\sqrt{2}} \left[\frac{1}{f_o^2} - \frac{\sigma_{\phi R}^2}{f_c^2} \right]^{-1/2} \tag{C-9}$$

$$f_2' = F \left[\frac{1}{f_o^2} - \frac{\sigma_{\phi R}^2}{f_c^2} \right]^{-1/2} \tag{C-10}$$

where

$$F = 1 + 0.038R^{-2.4} \quad , \quad R \leq 0.5$$

$$F = 1 + 0.14R^{-0.5} \quad , \quad R > 0.5$$

$$R = z_f / z_s$$

are the correct terms to be used in the generalized power spectra. $\sigma_{\phi R}^2$ the Rayleigh phase variance, was defined in Appendix B. The correction factor, F, was derived in Appendix D to correct for the finite structured layer thickness, z_s.

APPENDIX D

THE EFFECT OF FINITE SCATTERING LAYER THICKNESS ON THE MUTUAL COHERENCE FUNCTION

Following and expanding on Sreenivasiah,[D-1] the mutual coherence function of the signal for isotropic fluctuations around the propagation line of sight can be written as

$$G(p,\Delta f) = f(\eta)\exp\left[-\frac{\sigma_\phi^2}{2}\left(\frac{\Delta f}{f_c}\right)^2 - g(\eta)x^2\right] \qquad \text{(D-1)}$$

where

$$\eta = \left[\frac{\pi\Delta f}{K^2 c L_x^2}\frac{d\sigma_\phi^2}{dz}\right]^{1/2} z$$

$$x^2 = \left[\frac{K^2 c}{\pi\Delta f L_x^2}\frac{d\sigma_\phi^2}{dz}\right]^{1/2} p^2$$

$$\sigma_\phi^2 >> 1$$

$$n \geq 2$$

$$\frac{d\sigma_\phi^2}{dz} = \text{a constant in the scattering layer}$$

$$L_x^2 = L_y^2$$

$$L_{xy} = 0$$

The equations for $f(\eta)$ and $g(\eta)$ are

$$\frac{dg}{d\eta} = 4ig^2 + 1 - \frac{2g}{\eta} \qquad \text{(D-2)}$$

$$\frac{df}{d\eta} = 4igf \qquad \text{(D-3)}$$

The various propagation cases can be parameterized by any two of the following three numbers.

$$R_1 = z_1/z_s$$

$$R_2 = (z_t - z_1)/z_s$$

$$R = z_f/z_s = R_1R_2/(R_1+R_2)$$

z_1 is the coordinate of the center of the layer. Equations D-2 and D-3 were solved by a combination of analytic and numerical techniques for the values of R_1 and R_2 shown in Figure D-1. The results show that $G(p,\Delta f)$ can be well represented by

$$G(p,\Delta f) \approx \frac{\exp(iG\Delta f/f_2')}{(1-i\Delta f/Ff_2')} \exp\left[-\frac{\sigma_\phi^2}{2}\left(\frac{\Delta f}{f_c}\right)^2 - \left(\frac{p^2}{\ell_0^2}\right)\left(\frac{1}{1-i\Delta f/Ff_2'}\right)\right] \qquad \text{(D-4)}$$

where

$$f_2' = \frac{K^2 c L_x^2}{4\pi\sigma_\phi^2 z_f B_n}$$

$$F = 1 + 0.038R^{-2.4} \quad , \quad R \le 0.5$$

$$F = 1 + 0.14R^{-0.5} \quad , \quad R > 0.5$$

Equation D-4 is identical with Equation 42 in the text except for the F and G corrections. The G term can be ignored as it represents a uniform time shift.

Figures D-2 through D-11 compare the solutions for $G(p,\Delta f)$ (symbols) with Equation D-4 (solid curves). The excellent agreement is evident. Figure D-12 plots the correction factor, F, as a function of R that best corrects Equation D-4.

D-1 Sreenivasiah, I., et al., "Two-Frequency Mutual Coherence Function and Pulse Propagation in a Random Medium: An Analytic Solution to the Plane Wave Case," Radio Science, Vol. 11, Number 10, 775-778, October 1978.

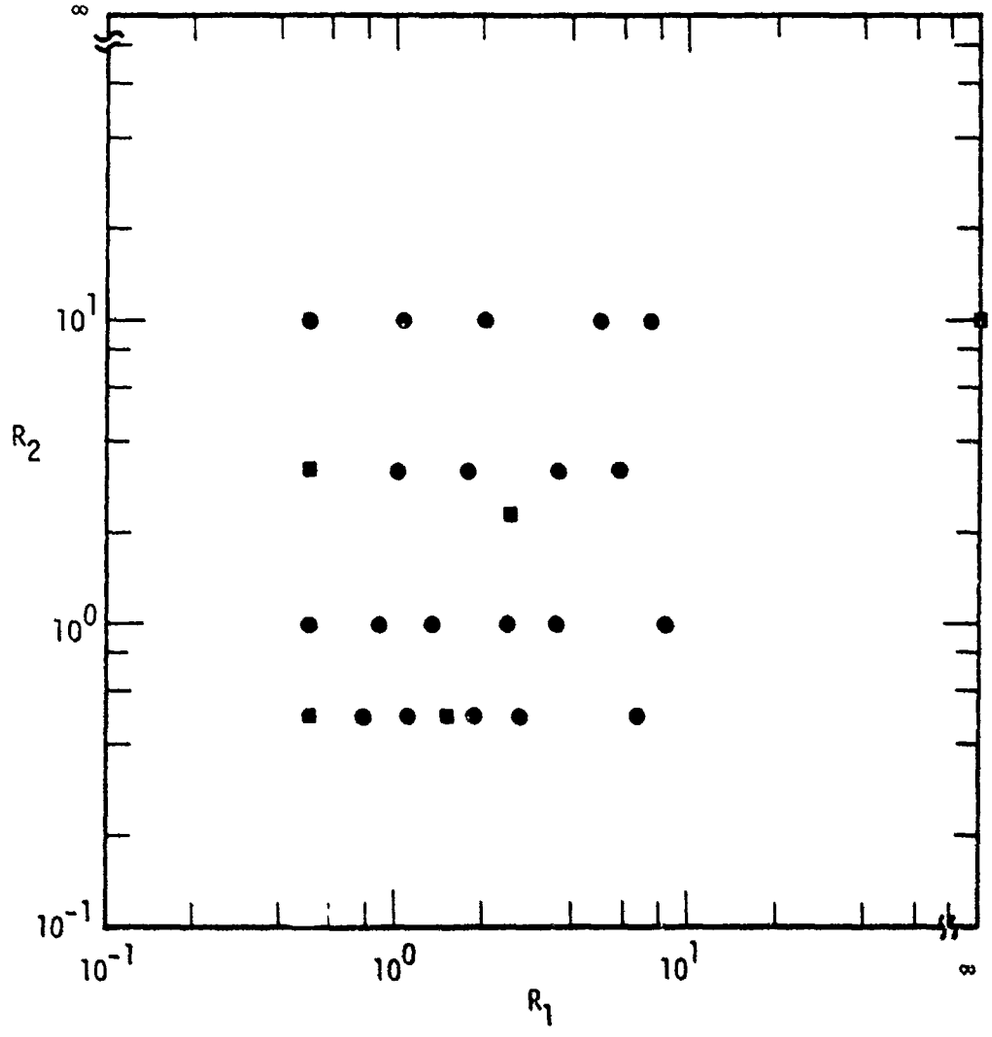

Figure D-1. Values of R_1 and R_2 for which Equations D-2 and D-3 are solved.

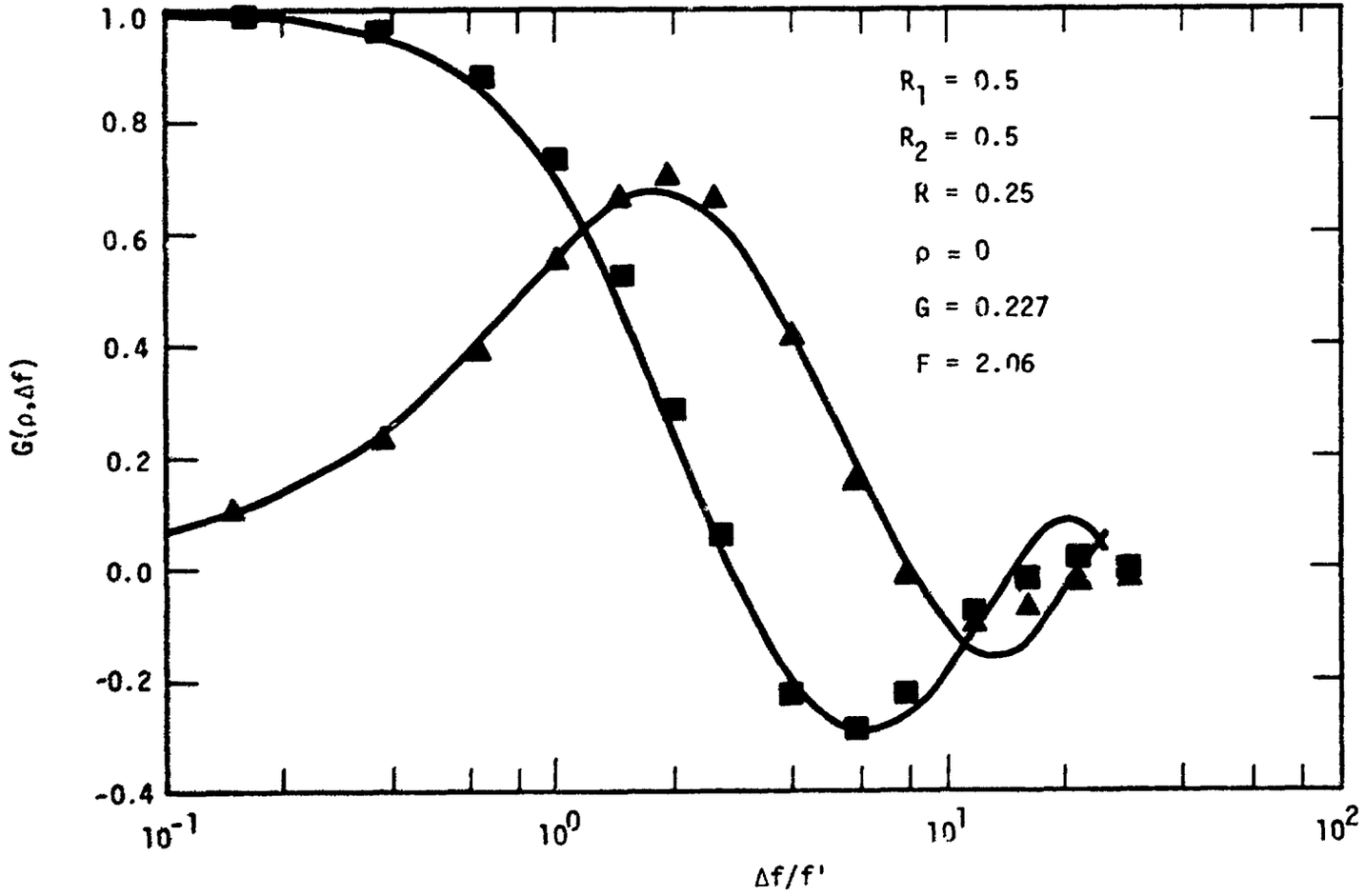

Figure D-2. Comparison of mutual coherence functions.

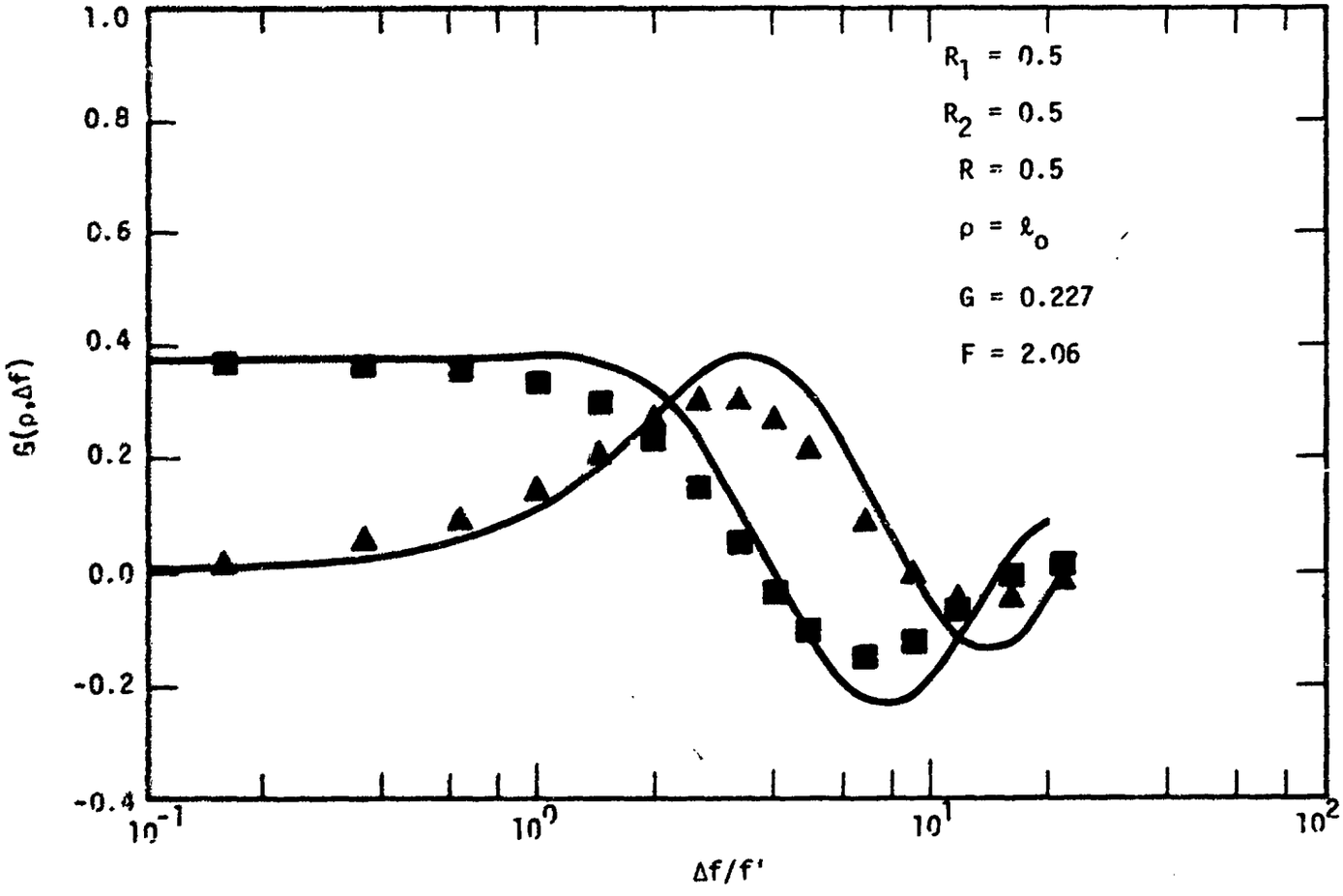

Figure D-3. Comparison of mutual coherence functions.

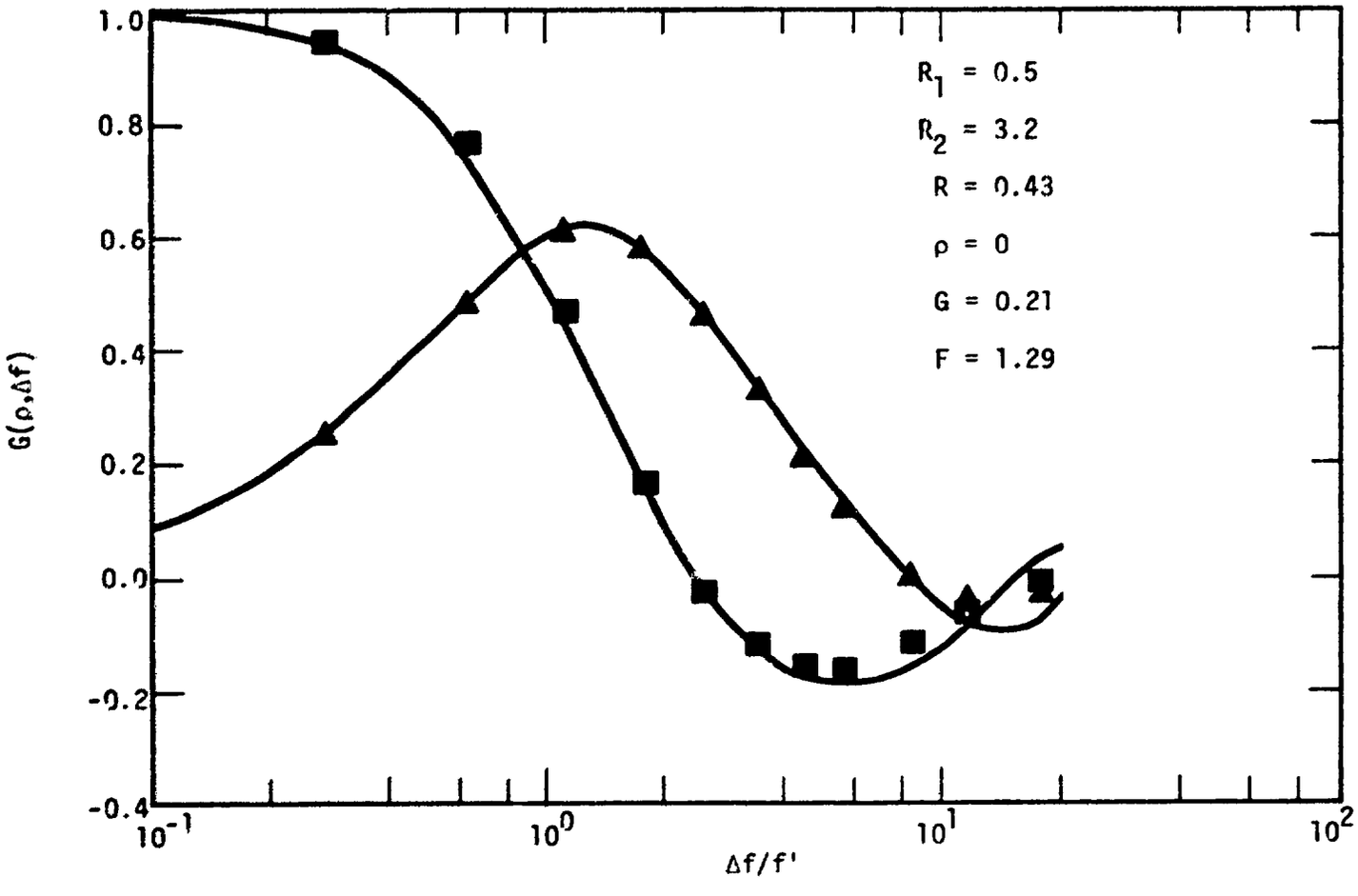

Figure D-4. Comparison of mutual coherence functions.

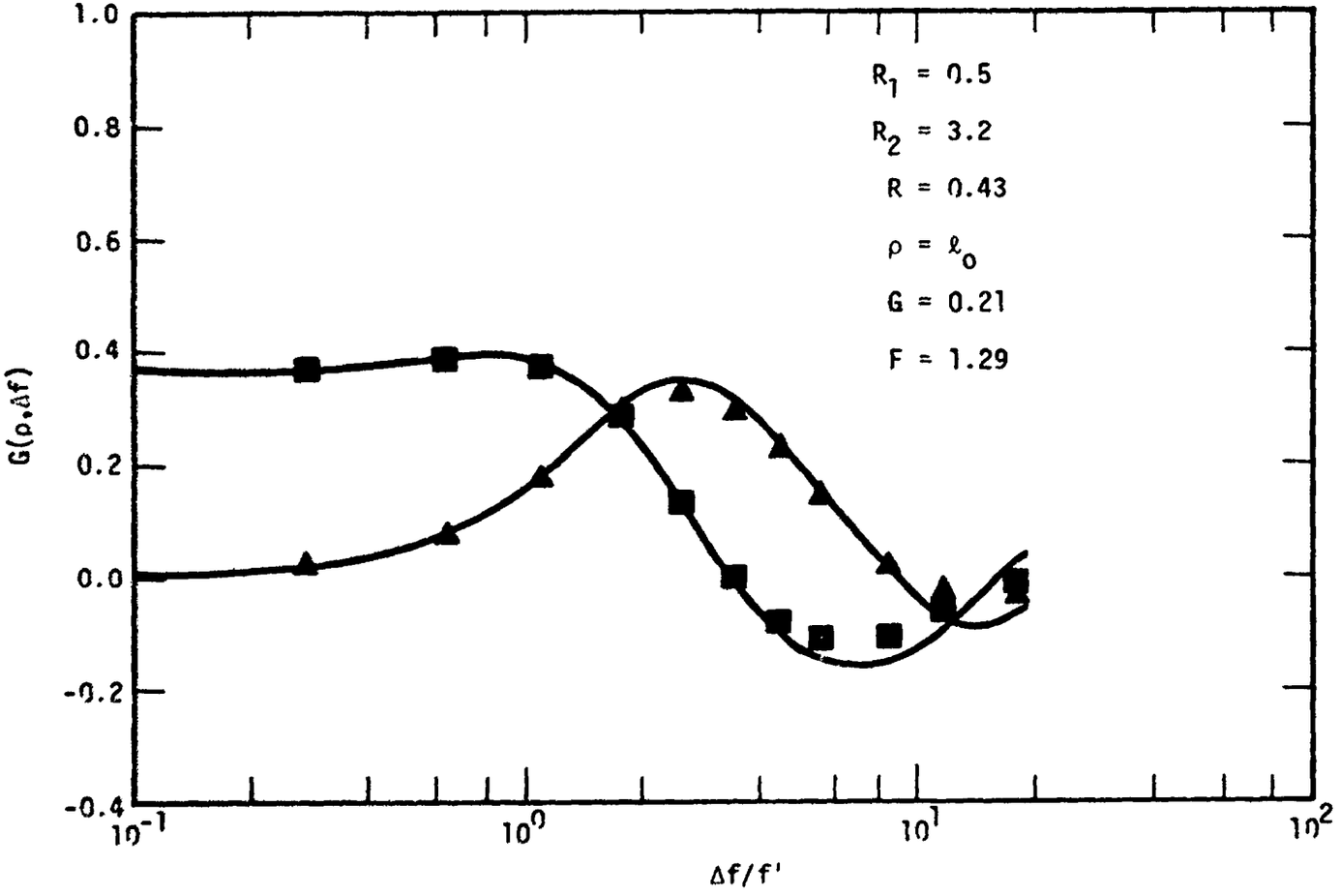

Figure D-5. Comparison of mutual coherence functions.

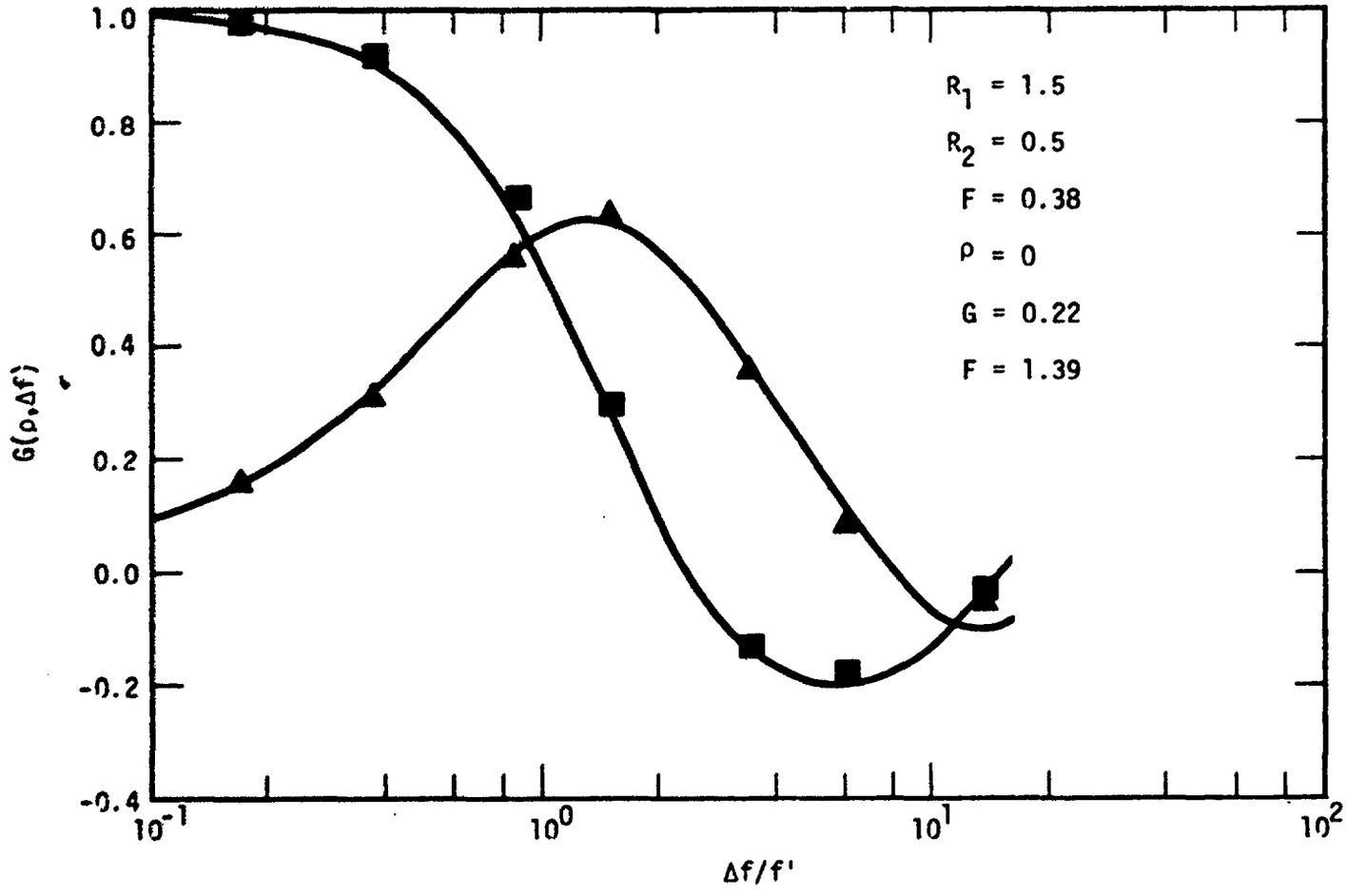

Figure D-6. Comparison of mutual coherence functions.

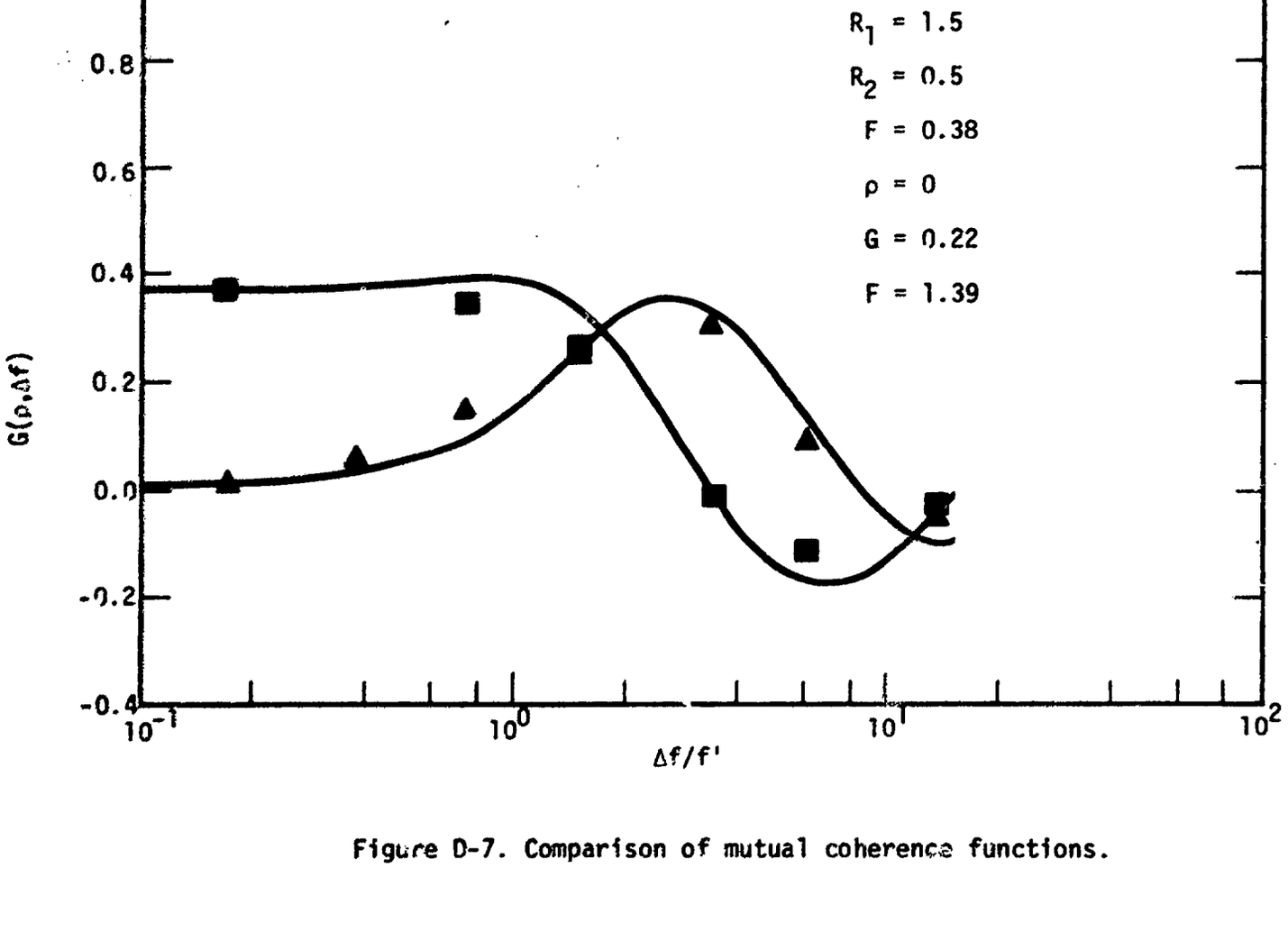

Figure D-7. Comparison of mutual coherence functions.

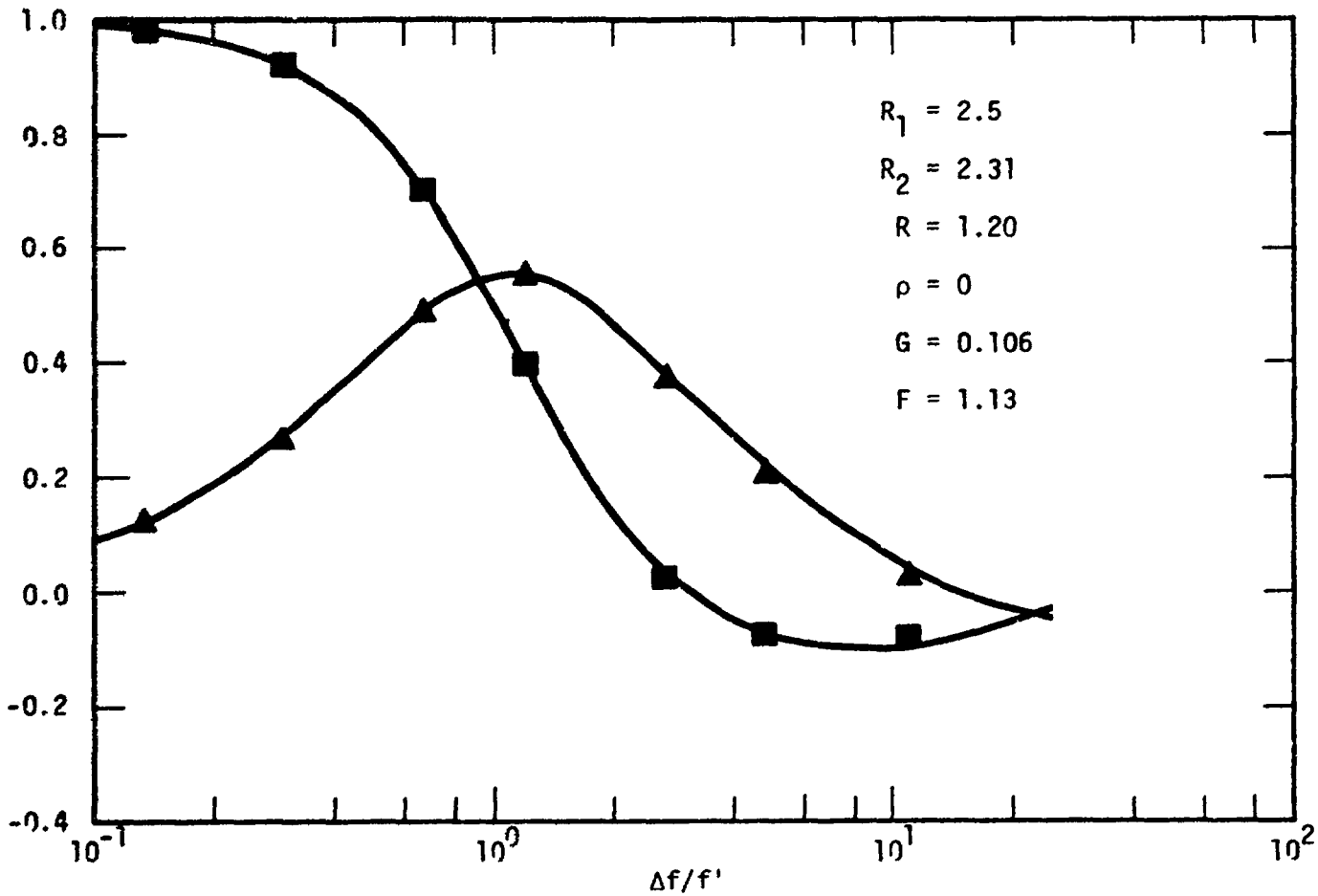

Figure D-8. Comparison of mutual coherence functions.

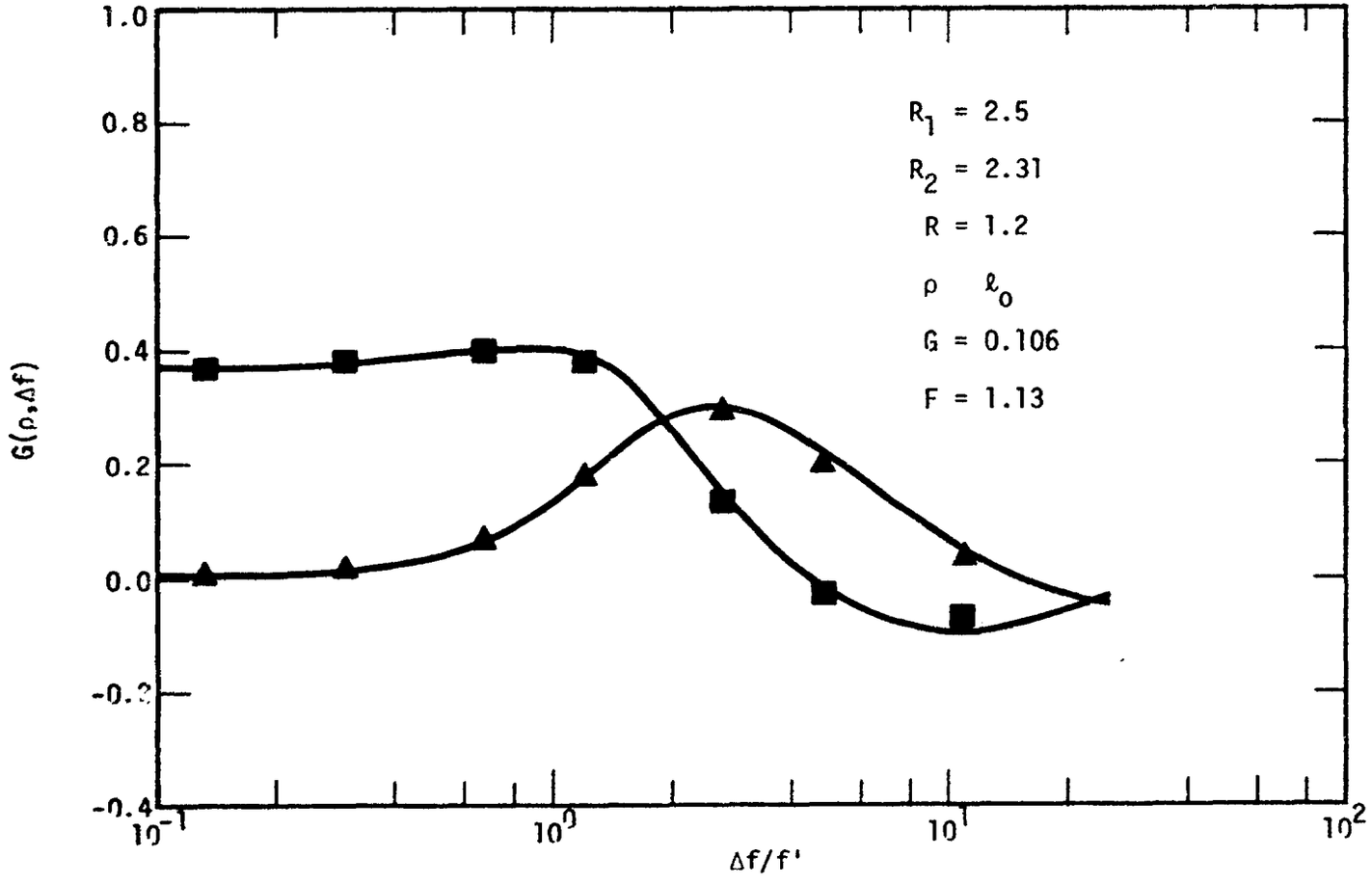

Figure D-9. Comparison of mutual coherence functions.

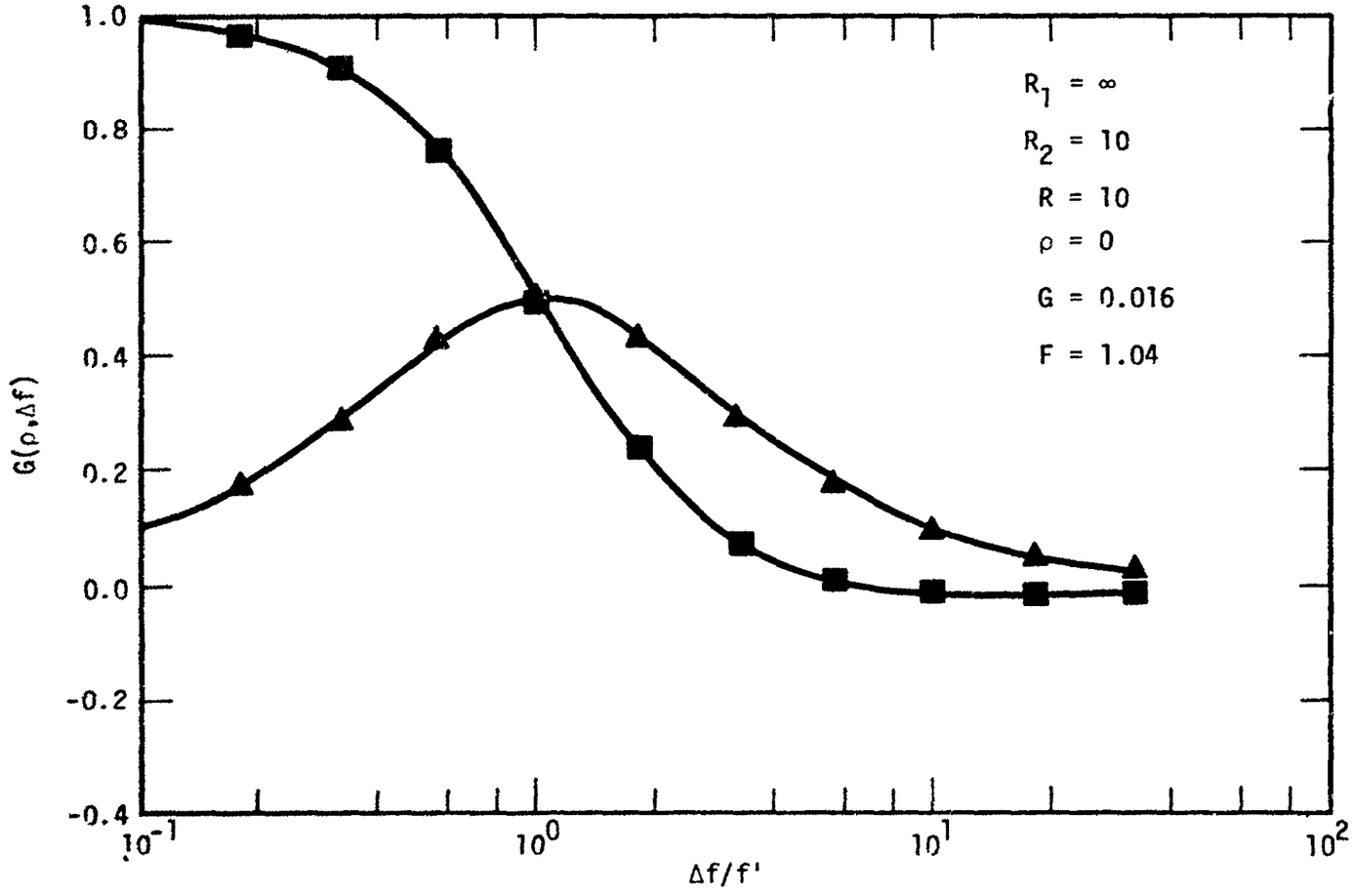

Figure D-10. Comparison of mutual coherence functions.

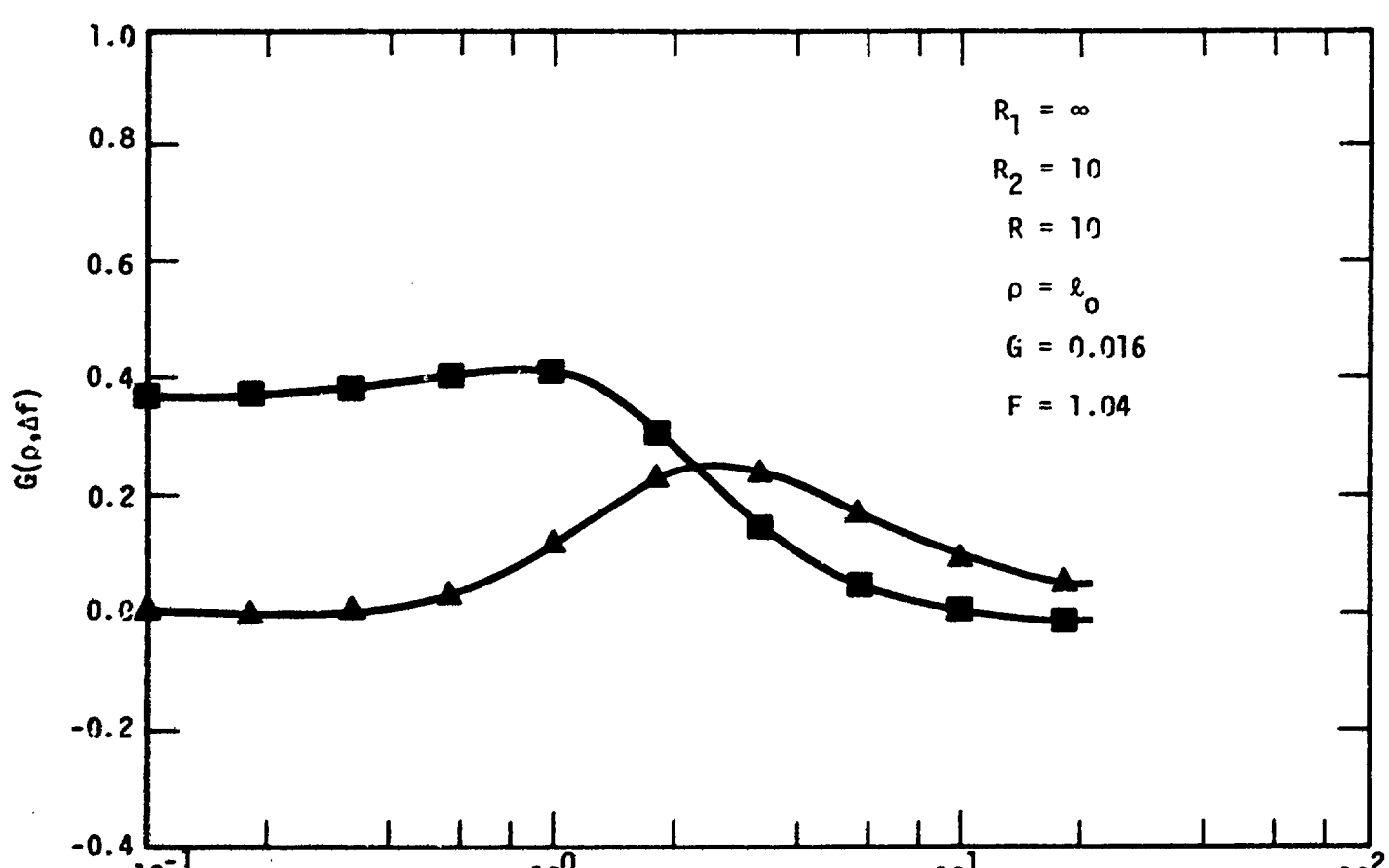

Figure D-11. Comparison of mutual coherence functions.

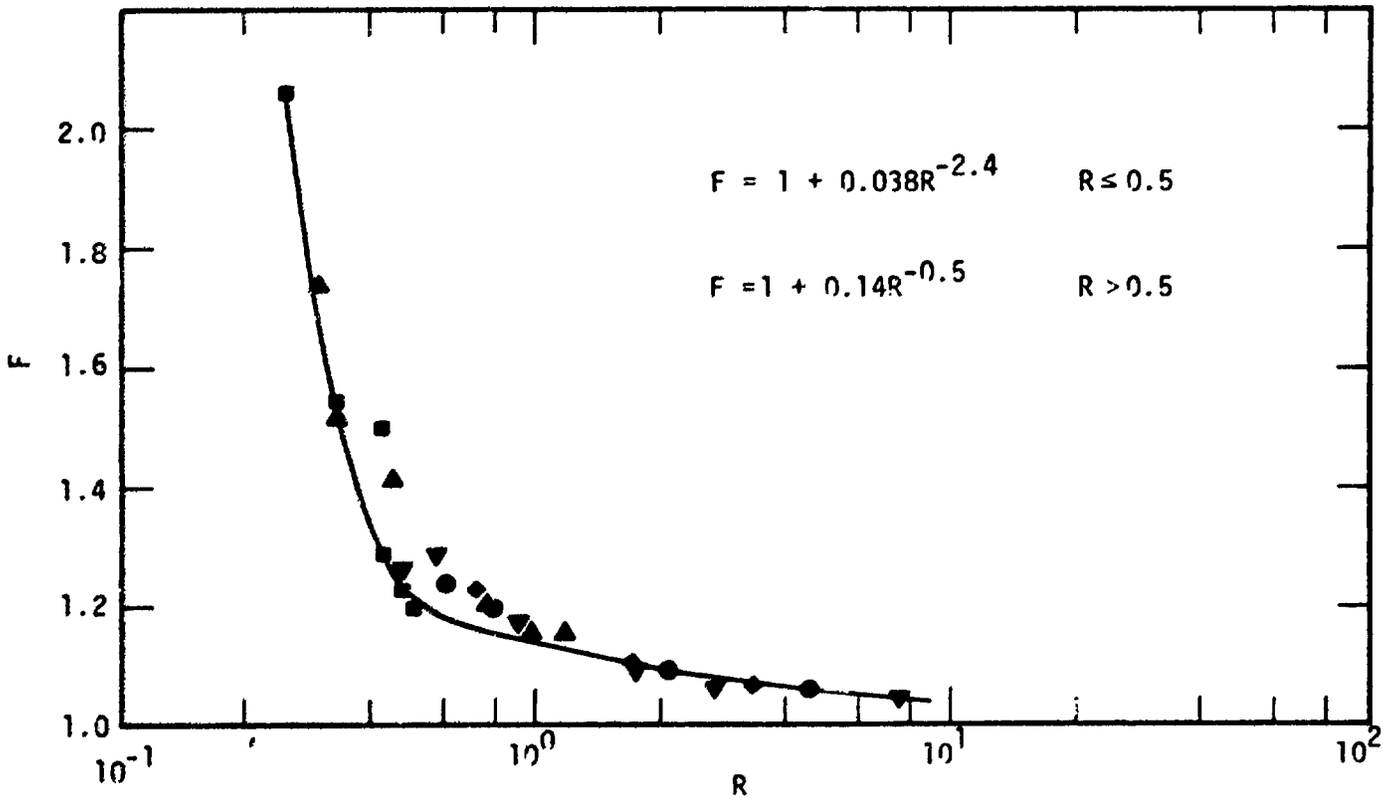

Figure D-12. Comparison of mutual coherent functions.

APPENDIX E

GENERATION OF EXPLICIT SAMPLES OF RAYLEIGH SCINTILLATED SIGNALS

The statistics of the signal are represented by the generalized power spectrum, $\Gamma(f,\tau)$, which is an implicit function of f', $\sigma_{\phi R}$, and τ_o. Since the process represented by $\Gamma(f,\tau)$ is stationary, $\Gamma(f,\tau)$ can be thought of as a colored noise spectrum. This means that samples of the signals can be generated parametric in delay, τ. Let a signal sample, for τ_i delay, be

$$U(t,\tau_i) = \frac{1}{2T} \sum_{n=-N}^{N} C_n(\tau_i)\, e^{i\frac{n\pi t}{T}} \qquad \text{(E-1)}$$

where $2T$ is the length of the sample and the range of t is $-T \le t \le T$. $2N$ is the number of discrete frequency points. Let

$$T > 100\ \tau_o$$

$$T/N < \tau_o/10$$

The Fourier coefficients in E-1 can then be assumed zero mean, independent, and gaussian distributed variables with a variance of

$$\overline{C_n^*(\tau_i)C_n(\tau_i)} = \left(\frac{2T}{\Delta\tau}\right)^2 \int_{\tau_i-\Delta\tau/2}^{\tau_i+\Delta\tau/2} d\tau \int_{(n-1/2)/2T}^{(n+1/2)/2T} df\ \Gamma(f,\tau) \qquad \text{(E-2)}$$

where $\Delta\tau$ is the delay resolution element.

Each Fourier coefficient can be sampled by

$$C_n(\tau_i) = \overline{C_n^*(\tau_i)C_n(\tau_i)}^{1/2} [-\ell n(R_1)]^{1/2} e^{i2\pi R_2} \qquad \text{(E-3)}$$

where R_1 and R_2 are two random numbers from a distribution whose elements are uniformly distributed between zero and one. The sample signal of delay τ_i is found by evaluating Equation E-1. This process is repeated for all τ_i. For many applications this may be the final step because $U(t,\tau_i)$ is also a sample of the channel impulse response function.

A special sampling case occurs in flat fading where the signal delay is small compared to the symbol period. The τ_i argument in Equation E-1 can be dropped. The variance of the coefficents are

$$\overline{C_n^* C_n} = (2T)^2 \int_{(n-1/2)/2T}^{(n+1/2)/2T} df \int_{-\infty}^{\infty} d\tau \Gamma(f,\tau) \qquad \text{(E-4)}$$

The coefficients are sampled by Equation E-3.

DISTRIBUTION LIST

DEPARTMENT OF DEFENSE

Assistant Secretary of Defense
Comm, Cmd, Cont & Intell
ATTN: C3IST&CCS, M. Epstein
ATTN: Dir of Intelligence Systems, J. Babcock

Defense Advanced Rsch Proj Agency
ATTN: TIO

Defense Communications Engineer Center
ATTN: Code R410, R. Craighill
ATTN: Code R123

Defense Nuclear Agency
4 cy ATTN: TITL
3 cy ATTN: RAAE

Defense Technical Information Center
12 cy ATTN: DD

Field Command
Defense Nuclear Agency
ATTN: FCPR

Field Command
Defense Nuclear Agency
ATTN: FCPRL

WWMCCS System Engineering Org
ATTN: R. Crawford

DEPARTMENT OF THE ARMY

Atmospheric Sciences Laboratory
U.S. Army Electronics R & D Command
ATTN: DELAS-EO, F. Niles

BMD Advanced Technology Center
Department of the Army
ATTN: ATC-T, M. Capps
ATTN: ATC-R, D. Russ
ATTN: ATC-O, W. Davies

BMD Systems Command
Department of the Army
ATTN: BMDSC-HW

Harry Diamond Laboratories
Department of the Army
ATTN: DELHD-N-P
ATTN: DELHD-N-P, F. Wimenitz
ATTN: DELHD-I-TL, M. Weiner

U.S. Army Nuclear & Chemical Agency
ATTN: Library

U.S. Army Satellite Comm Agency
ATTN: Document Control

DEPARTMENT OF THE NAVY

Naval Electronic Systems Command
ATTN: PME 117-20
ATTN: Code 501A
ATTN: PME 117-211, B. Kruger
ATTN: PME-117-2013, G. Burnhart

DEPARTMENT OF THE NAVY (Continued)

Naval Research Laboratory
ATTN: Code 4780, S. Ossakow
ATTN: Code 4700, T. Coffey

Strategic Systems Project Office
Department of the Navy
ATTN: NSP-43
ATTN: NSP-2722, F. Wimberly

DEPARTMENT OF THE AIR FORCE

Air Force Geophysics Laboratory
ATTN: OPR, A. Stair
ATTN: OPR, H. Gardiner
ATTN: PHI, J. Buchau
ATTN: PHP, J. Mullen

Air Force Weapons Laboratory
Air Force Systems Command
ATTN: DYC
ATTN: SUL

Air Force Wright Aeronautical Laboratories
ATTN: AAD, W. Hunt
ATTN: A. Johnson

Headquarters Space Division
Air Force Systems Command
ATTN: SKA, M. Clavin
ATTN: SZJ
ATTN: SZJ, W. Mercer
ATTN: YA, E. Butt

Strategic Air Command
ATTN: XPFS
ATTN: NRT

OTHER GOVERNMENT

Institute for Telecommunications Sciences
National Telecommunications & Info Admin
ATTN: W. Utlaut

DEPARTMENT OF ENERGY CONTRACTORS

Lawrence Livermore National Laboratory
ATTN: Doc Con for L-31, R. Hager
ATTN: Doc Con for L-389, R. Ott

Los Alamos National Scientific Laboratory
ATTN: Doc Con for E. Jones
ATTN: Doc Con For D. Simons
ATTN: Doc Con for MS 664, J. Zinn
ATTN: MS 670, J. Hopkins

Sandia National Laboratories
ATTN: Doc Con for Org 1250, W. Brown
ATTN: Doc Con for Org 4241, T. Wright

DEPARTMENT OF DEFENSE CONTRACTORS

Aerospace Corp.
ATTN: D. Olsen
ATTN: N. Stockwell
ATTN: V. Josephson

DEPARTMENT OF DEFENSE CONTRACTORS (Continued)

Berkeley Research Associates, Inc.
ATTN: J. Workman

ESL, Inc.
ATTN: J. Marshall

General Electric Co.
Space Division
ATTN: A. Harcar
ATTN: M. Bortner

General Electric Co.-TEMPO
ATTN: W. McNamara
ATTN: W. Knapp
ATTN: M. Stanton
ATTN: T. Stevens
ATTN: DASIAC

General Research Corp.
ATTN: J. Ise, Jr.
ATTN: J. Garbarino

GTE Sylvania, Inc.
Electronics Systems Grp-Eastern Div
ATTN: M. Cross

HSS, Inc.
ATTN: D. Hansen

Institute for Defense Analyses
ATTN: E. Bauer

JAYCOR
ATTN: S. Goldman

M.I.T. Lincoln Lab
ATTN: D. Towle

Mission Research Corp.
ATTN: R. Hendrick
ATTN: R. Kilb
ATTN: D. Sappenfield
ATTN: S. Gutsche
ATTN: D. Sowle
ATTN: F. Fajen
ATTN: R. Bogusch

DEPARTMENT OF DEFENSE CONTRACTORS (Continued)

Mitre Corp.
ATTN: B. Adams

Physical Dynamics, Inc.
ATTN: E. Fremouw

R & D Associates
ATTN: W. Karzas
ATTN: R. Lelevier
ATTN: B. Gabbard
ATTN: C. MacDonald
ATTN: F. Gilmore
ATTN: P. Haas

R & D Associates
ATTN: B. Yoon

Rand Corp.
ATTN: C. Crain
ATTN: E. Bedrozian

Science Applications, Inc.
ATTN: D. Hamlin
ATTN: J. McDougall
ATTN: L. Linson
ATTN: D. Sachs

Science Applications, Inc.
ATTN: J. Cockayne

SRI International
ATTN: W. Jaye
ATTN: G. Smith
ATTN: W. Chesnut
ATTN: R. Leadabrand
ATTN: C. Rino
ATTN: M. Baron

Technology International Corp.
ATTN: W. Boquist

Teledyne Brown Engineering
ATTN: R. Deliberis

Visidyne, Inc.
ATTN: J. Carpenter
ATTN: C. Humphrey